Journal of Medicinal Chemistry

Freie Universität Berlin

Subscriber access provided by UB + Fachbibliothek Chemie | (FU-Bibliothekssystem)

Article

Discovery of G Protein-Biased Dopaminergics with a Pyrazolo[1,5-*a*]pyridine Substructure

Dorothee Möller, Ashutosh Banerjee, Taygun C. Uzuneser, Marika Skultety, Tobias Huth, Bianca Plouffe, Harald Hübner, Christian Alzheimer, Kristina Friedland, Christian P. Müller, Michel Bouvier, and Peter Gmeiner

J. Med. Chem., **Just Accepted Manuscript** • DOI: 10.1021/acs.jmedchem.6b01857 • Publication Date (Web): 01 Mar 2017

ACS Publications

Journal of Medicinal Chemistry is published by the American Chemical Society. 1155 Sixteenth Street N.W., Washington, DC 20036

Discovery of G Protein-Biased Dopaminergics with a Pyrazolo[1,5-*a*]pyridine Substructure

*Dorothee Möller,[1] Ashutosh Banerjee,[1] Taygun C. Uzuneser,[2] Marika Skultety,[1] Tobias Huth,[3] Bianca Plouffe,[4] Harald Hübner,[1] Christian Alzheimer,[3] Kristina Friedland,[5] Christian P. Müller,[2] Michel Bouvier,[4] Peter Gmeiner[1]**

[1]Department of Chemistry and Pharmacy, Medicinal Chemistry, Friedrich-Alexander University Erlangen-Nürnberg, Schuhstraße 19, 91052 Erlangen, Germany

[2]Department of Psychiatry and Psychotherapy, Friedrich-Alexander University Erlangen-Nürnberg, Schwabachanlage 6, 91054 Erlangen, Germany

[3]Institute of Physiology and Pathophysiology, Friedrich-Alexander University Erlangen-Nürnberg, Universitätsstraße 17, 91054 Erlangen, Germany

[4]Institute for Research in Immunology and Cancer (IRIC), Department of Biochemistry and Molecular Medicine, University of Montreal, Québec, Canada H3C 1J4

[5]Department of Chemistry and Pharmacy, Molecular and Clinical Pharmacy, Friedrich-Alexander University Erlangen-Nürnberg, Cauerstraße 4, 91058 Erlangen, Germany

KEYWORDS:

GPCR, dopamine receptor, functional selectivity, ligand bias, G protein, β-arrestin, GIRK

ABSTRACT

1,4-Disubstituted aromatic piperazines are privileged structural motifs recognized by aminergic G protein-coupled receptors. Connection of a lipophilic moiety to the arylpiperazine core by an appropriate linker represents a promising concept to increase binding affinity and to fine-tune functional properties. In particular, incorporation of a pyrazolo[1,5-*a*]pyridine heterocyclic appendage led to a series of high affinity dopamine receptor partial agonists. Comprehensive pharmacological characterization involving BRET biosensors, binding studies, electrophysiology and complementation-based assays revealed compounds favoring activation of G proteins (preferably G_o) over β-arrestin recruitment at dopamine D_2 receptors. The feasibility to design G protein-biased partial agonists as putative novel therapeutics was demonstrated for the representative 2-methoxyphenylpiperazine **16c**, which unequivocally displayed antipsychotic activity *in vivo.* Moreover, combination of the pyrazolo[1,5-*a*]pyridine appendage with a 5-hydroxy-N-propyl-2-aminotetraline unit led to balanced or G protein-biased dopaminergic ligands depending on the stereochemistry of the head group, illustrating the complex structure-functional selectivity relationships at dopamine D_2 receptors.

INTRODUCTION

In recent years, a number of studies have identified 1,4-disubstituted aromatic piperazines (1,4-DAPs) as privileged scaffolds[1] interacting with aminergic G protein-coupled receptors (GPCRs), especially those belonging to the serotonergic, α-adrenergic and dopamine D_2 receptor (D_2R) family.[2, 3] Consisting of an aromatic head group in vicinity to a basic amine, they are able to recognize a three-dimensional pattern of highly conserved amino acids in the orthosteric binding pocket, a cavity formed within the helix bundle of the 7-transmembrane receptor (7-TM). 1,4-DAPs are able to mimic the crucial interactions between dopamine and the receptor and can therefore serve as surrogates for the endogenous agonist. Although the core region of the aromatic piperazines is sufficient to allow binding to D_2R and the closely related D_3R subtype,[4] enlargement of the chemical structures by addition of a flexible linker and a second, mostly lipophilic system (type I compounds, Figure 1) has been found to promote enhanced affinity and subtype selectivity.[2, 4, 5]

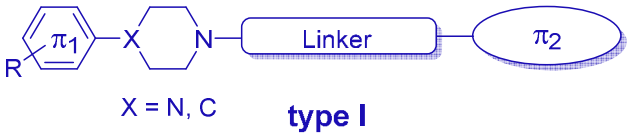

Figure 1. Chemical structure of type I compounds (1,4-DAP) consisting of an aromatic core structure (π_1), a basic amine unit, a linker region and a second, mostly lipophilic system (π_2).

The relevance of type I compounds is best illustrated by the growing number of antipsychotic drugs with antagonist/partial agonist activity at D_2R and D_3R. Besides aripiprazole[6] (**1a**), cariprazine[7] (**1b**) and brexiprazole[8] (**1c**) have recently received FDA-approval for the treatment of schizophrenia and bipolar I manic/mixed episodes or major depressive disorders, respectively (Figure 2).[9]

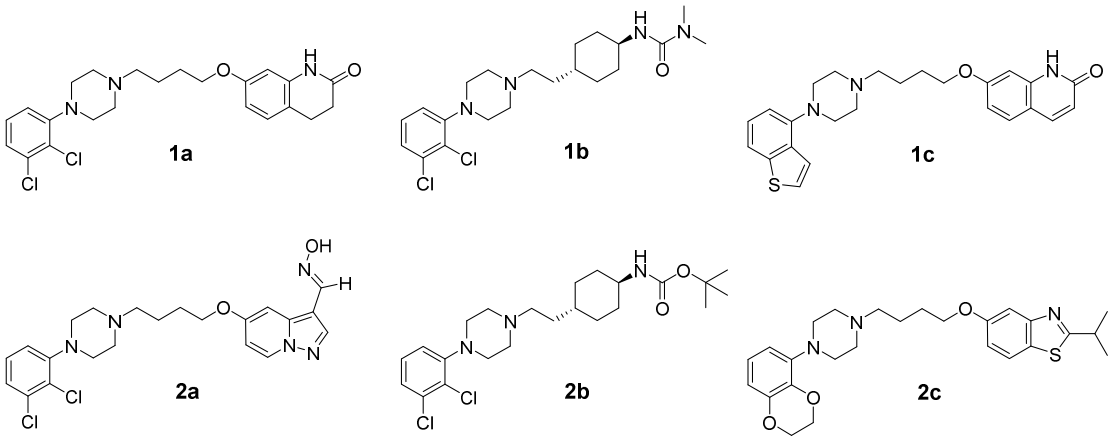

Figure 2. Chemical structures of approved antipsychotics drugs **1a-c** and recently described functionally selective dopamine receptor partial agonists (**2a-c**) bearing a 1,4-DAP as orthosteric head group.

Traditionally, different properties have been attributed to the three individual parts (orthosteric head group, linker and lipophilic appendage) of 1,4-DAPs. While the arylpiperazine including its substituents has been considered responsible for the intrinsic activity of a given ligand, the lipophilic appendage addressing a secondary binding pocket has been thought to promote enhanced affinity with the linker simultaneously controlling subtype-selectivity.[2] More recently, a number of compounds with an enlarged 1,4-DAP structure have been described (e.g. compounds **2a-c**, Figure 2), that are able to activate D_2R in a functionally selective manner.[3, 10-14] This behavior, also described as ligand bias, is the capacity of a ligand to direct the signaling of a GPCR to a preferential signal transducer while other signaling pathways remain largely unaffected.[15, 16] Interestingly, ligands preferably activating G protein-mediated signaling and those preferentially leading to a recruitment of β-arrestins have been found to share high chemical similarity.[10-13] This behavior has been attributed to a complex interplay between the orthosteric aromatic pharmacophores and the lipophilic appendages connected by an appropriate spacer, enabling the ligands to adopt a bitopic orthosteric/allosteric binding mode.[17-19] In 2014, we presented pyrazolo[1,5-*a*]pyridine heterocycles as valuable lipophilic moieties providing high D_2R/D_3R affinity, when attached to a 2,3-dichlorophenylpiperazine by a butoxy-linker. The ligands including the oxime

substituted-pyrazolo[1,5-*a*]pyridine **2a** (Figure 2) displayed partial agonist properties for G protein activation, while they were inhibitors for the recruitment of β-arrestin-2 at the D_2R, thus being high affinity biased agonists.[10] This finding was supported by a very recent report on G protein-biased agonists with a very similar structural architecture replacing the pyrazolo[1,5-*a*]pyridine moiety by a bioisosteric benzothiazole unit (compound **2c** and analogs).[12] Extending our previous investigations, we aimed at exploring the different effects of modifications in linker region as well as variation of the orthosteric recognition element. Thus, we replaced the 2,3-dichlorophenylpiperazine unit by a 2-methoxyphenylpiperazine group. Moreover, an exchange of the oxymethylene part of the linker by an aminocarbonyl group was investigated. To complement the phenylpiperazine-type head group by a classical dopamine bioisostere, we planned the incorporation of both enantiomeric forms of 5-hydroxy-*N*-propyl-2-aminotetraline, a conformationally restricted scaffold known for its agonist properties at D_2-like receptors.[20] Based on this comprehensive set of compounds, differential studies of signaling profiles and SAR studies should allow to identify molecular determinants of functional selectivity. Guided by the hypothesis that *in vitro* profiles similar to those of the approved drug **1a** should predict *in vivo* antipsychotic activity, we performed a proof of concept study in rats. Results indicate the feasibility of pyrazolo[1,5-*a*]pyridines as useful scaffolds for the development of functionally selective CNS drugs.

RESULTS

1a, an approved antipsychotic drug has been previously described as partial D_2R agonist, preferentially activating G protein-mediated pathways with either little or no efficacy for the recruitment of β-arrestin-2.[10, 12, 13, 21] Employing our recently described affinity-generating pyrazolo[1,5-*a*]pyridine moieties, we aimed at developing new, biased D_2R partial agonists with putative antipsychotic activity. The heterocyclic moieties were combined with different orthosteric dopamine surrogates using either butoxy- or butyramido-derived spacers, since ligand bias at D_2R results from a complex interplay between orthosteric

pharmacophores, linker regions and liphophilic moieties addressing a secondary binding pocket.[3, 10-14, 19]

5-Butyramido pyrazolo[1,5-*a*]pyridines. In a first series of derivatives, the highly flexible butoxy-linker connecting the orthosteric head group with the heterocyclic moiety was replaced by an amide-moiety, thereby ideally constraining the ligands into a bioactive conformation. The respective 5-butyramido-pyrazolo[1,5-*a*]pyridines were synthesized by a combination of two independently prepared building blocks (Scheme 1). For the synthesis of the orthosteric pharmacophore and linker region, two commercially available phenylpiperazines (2,3-dichloro- and 2-methoxyphenylpiperazine) were subjected to nucleophilic displacement reactions with methyl 4-bromobutyrate, leading to the methyl carboxylates **3a** and **3b**. Subsequent ester hydrolysis with sodium hydroxide in methanol/water resulted in formation of the sodium carboxylates **4a** and **4b**, which were isolated in excellent yield by precipitation.[22] Carboxylates **4a** and **4b** were activated using HATU and coupled to 5-aminopyrazolo[1,5-*a*]pyridine (**5**), which was synthesized in analogy to previously described protocols.[23, 24] While the resulting amides **6a** and **6b** represent target compounds on their own, previous studies suggested that the pyrazolo[1,5-*a*]pyridine scaffold can be further modified in position 3 to enhance affinity for D_2-like receptors.[10, 23, 25] Thus, the azaindoles **6a** and **6b** were reacted under Vilsmeyer conditions to yield the carbaldehydes **7a** and **7b**. Subsequent conversion into oxime derivatives was realized by refluxing with hydroxylamine hydrochloride in ethanol/water.[26] The oximes **8a** and **8b** were isolated as an inseparable 1:1 mixture of two isomers which were identified as (*E*) and s-cis/s-trans isomers by diagnostic NOESY experiments. Finally, the oximes were reacted with acetic acid anhydride under reflux conditions[27] or cyanuric chloride in DMF at room temperature[28, 29] to afford the carbonitriles **9a** and **9b**.

Scheme 1.† *Synthesis of pyrazolo[1,5-a]pyridine-derived dopaminergics containing an amide linker.*

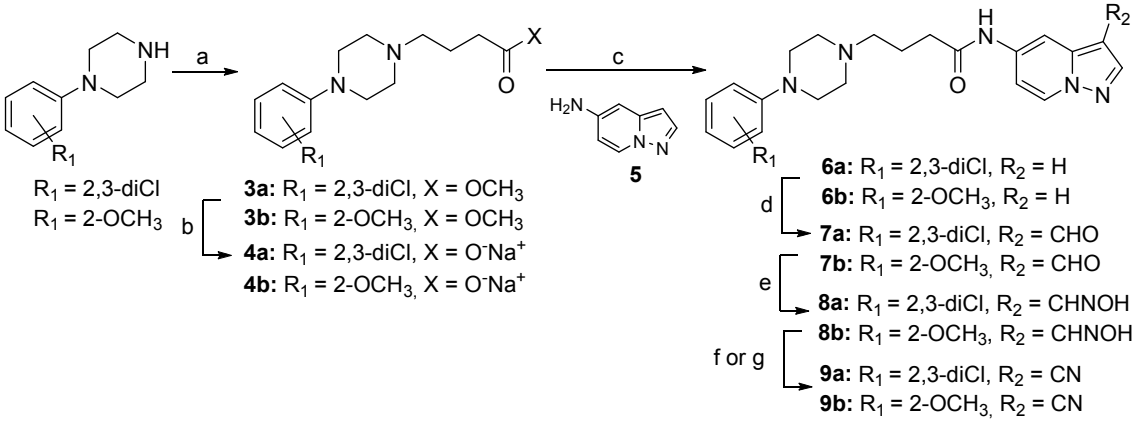

† Reagents and conditions: (a) methyl 4-bromobutyrate, TEA, DMF, rt, 24 h (88–98%); (b) 1 M NaOH, MeOH, 65 °C, 6 h (93–94%); (c) 5-aminopyrazolo[1,5-*a*]pyridine, HATU, DIPEA, DMF/CH_2Cl_2, 24h, rt (68–95%); (d) $POCl_3$, DMF, 0 °C to rt, 1 h (58–59%); (e) hydroxylamine · HCl, EtOH/H_2O, reflux, 2 h (77–83%); (f) for **9a** TCT, DMF, rt, 5 h (75%); (g) for **9b** Ac_2O, reflux, 6 h (12%).

Prior to functional characterizations, binding affinities of the newly synthesized compounds **6a**,**b**–**9a**,**b** were determined employing radioligand displacement studies with cell membranes expressing dopamine receptors or related receptors of interest (D_1R, $D_{2L}R$, $D_{2S}R$, D_3R, D_4R, 5-$HT_{1A}R$, 5-$HT_{2A}R$, α_1R, Table 1). For the entire set of test compounds, competition experiments revealed high binding affinities in the low nanomolar to subnanomolar range for the family of D_2-like receptors. Among the unmodified pyrazolo[1,5-*a*]pyridines **6a**,**b** and their formyl-substituted congeners **7a**,**b**, affinities were found to depend on the orthosteric phenyliperazine. Test compounds bearing the 2,3-dichlorophenylpiperazine moiety showed 5-fold higher affinity for $D_{2L}R$, $D_{2S}R$ and D_3R. Introduction of the formyl residue was beneficial for D_2R affinity, leading to subnanomolar K_i values at $D_{2L}R$ and $D_{2S}R$ for the carbaldehyde **7a** (0.30, 0.41 and 1.7 for $D_{2L}R$, $D_{2S}R$ and D_3R). Further modifications of the substituents only slightly influenced binding affinities for $D_{2L}R$, $D_{2S}R$, preserving the low nanomolar- to subnanomolar binding characteristics (0.50-1.11 nM for **8a**,**b** **9a**,**b** at $D_{2L}R/D_{2S}R$). Hence, formyl-, oxime- and cyano-substituted compounds displayed binding affinities for $D_{2L}R/D_{2S}R$ that are highly similar to those of the antipsychotic drug **1a** (K_i 0.54 and 0.45 nM for $D_{2L}R$ and $D_{2S}R$). Independent from the orthosteric phenylpiperazine and the

substitution pattern of the pyrazolo[1,5-*a*]pyridine appendage, target compounds displayed only small differences in their affinity for D_4R (K_i 8.1-34 nM) and for 5-$HT_{1A}R$ (K_i 21-40 nM). At the closely related 5-$HT_{2A}R$ subtype the 2,3-dichlorophenylpiperazines **6a-9a** showed low nanomolar affinity (K_i 2.6-6.3 nM), whereas affinities of the 2-methoxyphenylpiperazines **6b-9b** were roughly 50-fold lower (K_i 120-380 nM). While the compound family displayed week binding affinity (210-2900 nM) and hence selectivity over D_1R, all 5-butyramidopyrazolo[1,5-*a*]pyridines also had substantial affinity (1.6-10 nM) for α_1R.

Table 1. Binding affinities and functional properties of 5-butyramidopyrazolo[1,5-*a*]pyridines **6a**,**b**-**9a**,**b**.

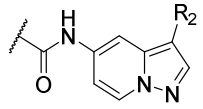

	1,4-DAP	R_2	K_i [nM]† hD_1‡	hD_{2L}§	hD_{2S}§	hD_3§	hD_4§	p5-HT_{1A}††	h5-HT_{2A}‡‡	$p\alpha_1$§§	[^{35}S]GTPγS $hD_{2S}/G\alpha_{oA}$ EC_{50}†††	E_{max}‡‡‡	$hD_3/G\alpha_{oA}$ EC_{50}†††	E_{max}‡‡‡
1a	2,3-diCl	-	310 ± 140	0.53 ± 0.24	0.45 ± 0.06	2.3 ± 1.2	81 ± 16	77 ± 22	3.7 ± 1.1	17 ± 0.71	39	67 ± 2	20	52 ± 3
6a	2,3-diCl	H	240 ± 0.0	8.1 ± 3.5	7.8 ± 2.1	5.6 ± 1.2	14 ± 3.1	23 ± 12	4.9 ± 2.1	7.5 ± 1.6	240	50 ± 2	45	65 ± 4
6b	2-MeO	H	1700 ± 840	46 ± 29	36 ± 24	97 ± 20	14 ± 5.1	31 ± 2.8	310 ± 0.0	5.3 ± 1.1	630	38 ± 3	66	45 ± 3
7a	2,3-diCl	CHO	210 ± 74	0.30 ± 0.12	0.41 ± 0.19	1.7 ± 0.56	30 ± 7.6	21 ± 2.8	6.3 ± 4.2	4.9 ± 0.56	13	43 ± 2	37	83 ± 3
7b	2-MeO	CHO	1200 ± 770	1.4 ± 0.43	1.5 ± 0.81	70 ± 35	34 ± 16	29 ± 18	300 ± 49	4.6 ± 1.0	150	41 ± 2	79	53 ± 4
8a	2,3-diCl	oxime	2900 ± 1900	0.57 ± 0.31	0.50 ± 0.14	2.2 ± 0.80	31 ± 14	27 ± 9.9	2.6 ± 1.0	10 ± 7.0	600	47 ± 3	3.8	74 ± 3
8b	2-MeO	oxime	900 ± 560	0.97 ± 0.62	0.52 ± 0.05	13 ± 4.6	8.1 ± 1.9	22 ± 7.1	120 ± 7.1	1.6 ± 1.1	470	37 ± 3	38	58 ± 3
9a	2,3-diCl	CN	250 ± 100	0.91 ± 0.58	0.52 ± 0.11	2.3 ± 0.08	32 ± 6.1	40 ± 4.2	5.6 ± 1.7	8.5 ± 2.2	870	50 ± 4	62	83 ± 4
9b	2-MeO	CN	860 ± 630	1.1 ± 0.73	0.55 ± 0.17	28 ± 12	17 ± 4.1	16 ± 1.4	380 ± 21	2.0 ± 0.14	84	32 ± 2	42	57 ± 4

†Data represent mean ± S.D. of two to six independent experiments, each performed in triplicate. Radioligands: ‡[^{3}H]SCH23990, §[^{3}H]spiperone, ††[^{3}H]WAY100635, ‡‡[^{3}H]ketanserin, §§[^{3}H]prazosin. ††† Potency given in nM. ‡‡‡ Efficacy normalized to the reference agonist quinpirole (100%) and buffer (0%). Data represent mean ± S.E.M. from the pooled curve of four to seven individual experiments, each performed in triplicate.

To determine functional properties of the test compounds at the $G\alpha_{i/o}$-coupled $D_{2S}R$ and D_3R, we performed [^{35}S]GTPγS incorporation assays with membranes from transiently

transfected HEK293T cells. The ability of the ligands to stimulate nucleotide exchange was measured using $G\alpha_{oA}$ as representative G protein subunit, which is known to be activated by both, D_2R and D_3R.[30-33] For both subtypes the antipsychotic drug **1a** elicited submaximal responses (67 % and 52 % of the quinpirole effect at $D_{2S}R$ and D_3R, respectively), which is good agreement with its partial agonist nature (Table 1, Supplementary Figure 1a). Similar potencies of 39 nM at $D_{2S}R$ and 20 nM at D_3R were observed in the two test systems, indicating little preference for one receptor subtype over the other. In contrast, pyrazolo[1,5-*a*]pyridines **6a**,**b**, **7b**, **8a,b** and **9a**,**b** showed a preferential activation of $G\alpha_{oA}$ via D_3R over $D_{2S}R$ (Supplementary Figure 1b,c and 1e-i) with up to 150-fold higher potencies (EC_{50} 3.8-79 nM and 84-870 nM at D_3R and $D_{2S}R$, respectively) as well as higher efficacies (E_{max} 45-83% at D_3R vs. 32-50 % at $D_{2S}R$). Only the 2,3-dichlorphenyl-piperazine **7a** showed a slightly higher potency for the activation of $D_{2S}R$ (13 nM vs. 37 nM at D_3R, Supplementary Figure 1d). The closely related oxime **8a**, however, was the most potent activator of D_3R (EC_{50} 3.8 nM, E_{max} 83 %, Supplementary Figure 1f). Additionally, compounds **6a**,**b**-**9a**,**b** were examined for their capacity to promote recruitment of β-arrestin-2 to $D_{2S}R$. Similar to the reference antipsychotic **1a**, none of the pyrazolo[1,5-*a*]pyridines with amide-substructure induced a significant effect (Supplementary Figure 2a) when they were tested at a concentration of 10 μM in the PathHunter assay. This antagonism stands in contrast to the partial agonist properties observed in the [^{35}S]GTPγS binding experiments, identifying 1,4-DAPs with butyramido-spacer and a pyrazolo[1,5-*a*]pyridine appendage as G protein-biased ligands at D_2R. Compared to the functional properties of chemical analogs comprising a butoxy-spacer (e.g. the antipsychotic **1a**), inferior D_2R partial agonist properties (reduced potencies, efficacies, or both) were observed for **6a**,**b**-**9a**,**b**. In spite of their subnanomolar binding affinities reduction of the conformational flexibility by introduction of the amide-spacer did not prove successful in constraining the ligands in a bioactive conformation that fosters receptor activation.

Modification of the orthosteric recognition element. Complimentary to the modifications of the spacer region and the lipophilic appendage, we explored the effects of different aromatic head groups, which serve as primary recognition element for aminergic receptors.[2] While previous studies have widely used 2,3-dichlorophenylpiperazines as dopamine surrogate,[10, 13] we employed closely related 2-methoxyphenylpiperazines but also more divergent 5-hydroxy-*N*-propyl-2-aminotetralines, rigidized dopamine scaffolds known for their D_2R-agonist properties.[20]

Scheme 2.† Synthesis of pyrazolo[1,5-*a*]pyridine-derived dopaminergics containing a butoxy-linker.

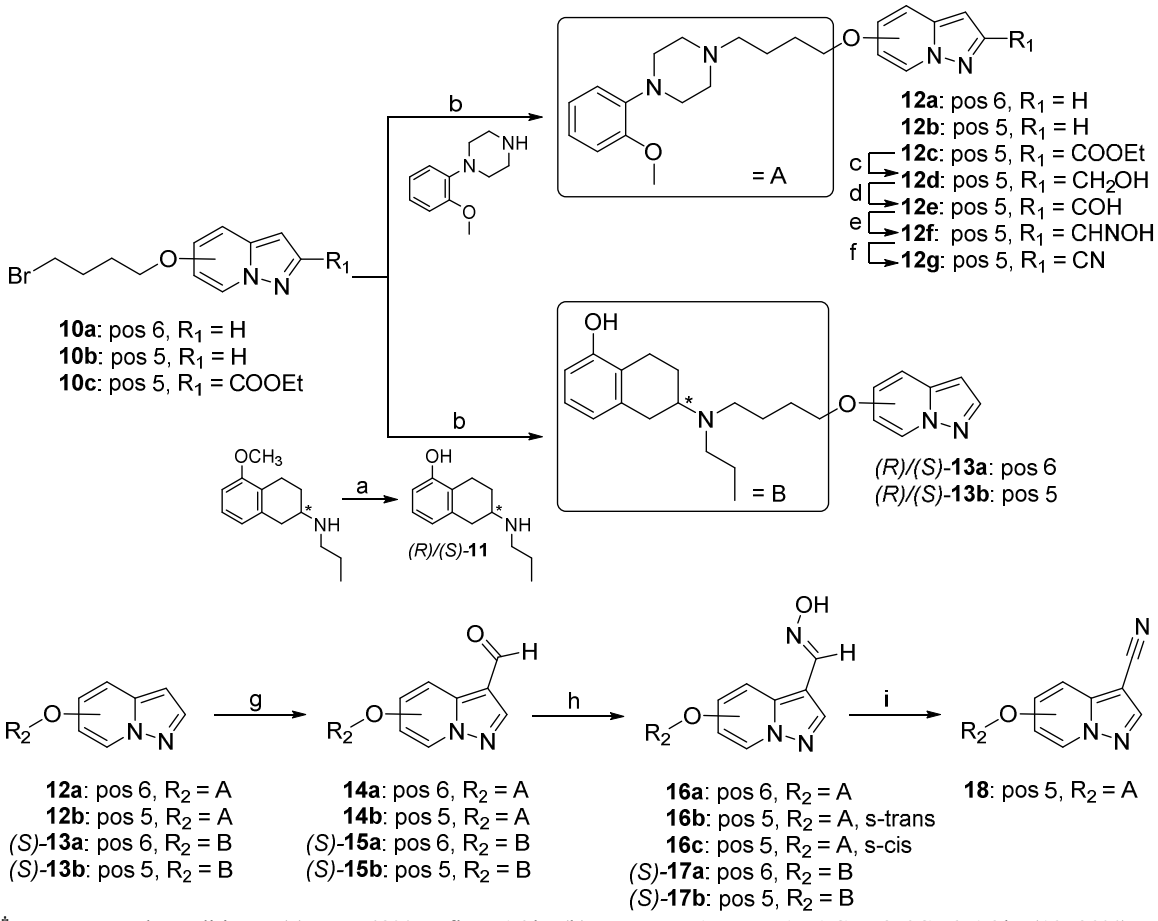

† Reagents and conditions: (a) HBr 48%, reflux, 16 h; (b) KI, DIPEA or TEA, ACN, 85°C, 6–16 h, (19–89%); (c) $LiAlH_4$, Et_2O, 0 °C to rt, 1 h (74%), (d) MnO_2, CH_2Cl_2, rt, 14 h (97%); (e) hydroxylamine hydrochloride, EtOH/H_2O, reflux, 2 h (85%); (f) TCT, DMF, rt, 7 h (54%). (g) $POCl_3$, DMF, 0 °C to rt, 1 h (79–98%); (h) hydroxylamine · HCl, EtOH/H_2O, reflux, 2 h (35–89%); (i) Ac_2O, reflux, 6 h (79%).

Synthesis of target compounds was accomplished starting from either commercially available 2-methoxyphenylpiperazine or (*R*)/(*S*)-5-methoxy-*N*-propyl-2-aminotetraline, which

was transformed into the phenol (*R*)/(*S*)-**11** by refluxing in hydrobromic acid. Subsequent coupling to the pyrazolo[1,5-*a*]pyridine appendage was conducted by nucleophilic displacement reaction with 5- or 6-(4-bromo)butoxypyrazolo[1,5-*a*]pyridines **10a** or **10b**,[10] yielding target compounds **12a**,**b** and (*R*)/(*S*)-**13a**,**b**, respectively. In the same way, 2-substituted pyrazolo[1,5-*a*]pyridine **12c** was obtained starting from 2-methoxyphenylpiperazine and the 2-ethoxy-carbonylpyrazolo[1,5-*a*]pyridine derivative **10c**[10]. The ethyl-carboxylate **12c** was transformed into the primary alcohol **12d** using a solution of $LiAlH_4$ in diethyl ether. Reoxidation with manganese(IV) oxide afforded the aromatic aldehyde **12e** in excellent yield. The aldehyde could be converted to the aldehydoxime **12f** by treatment with hydroxylamine hydrochloride in aqueous ethanol. Subsequent reaction with cyanuric chloride in DMF[10] gave the carbonitrile **12g**. Since addition of polar substituents into position 3 of the pyrazolo[1,5-*a*]pyridine moiety has previously been shown to have beneficial effects on dopamine D_2R-like affinity,[10, 23] dopaminergics **12a**,**b** and (*S*)-**13a**,**b** were further functionalized in analogy to previously described procedures.[10, 23, 25] Introduction of formyl residues was realized by Vilsymeyer-type formylation affording target compounds **14a**,**b** and (*S*)-**15a**,**b** in good yields. The following conversion to the corresponding oximes by refluxing with an aqueous solution of hydroxylamine hydrochloride in ethanol led to a mixture of (*E*)-*s-cis/s-trans* configured isomers **16a-c**, (*S*)-**17a**,**b** which could only be separated in the case of the 5-butoxy-phenylpiperazines **16b**,**c**. For the latter, a final conversion into the corresponding 3-cyano-substituted pyrazolo[1,5-*a*]pyridine **18** was performed by refluxing in acetic acid anhydride.

Binding affinities. Affinities of target compounds **12a-g** to **18** for dopamine D_1R, $D_{2L}R$, $D_{2S}R$, D_3R and D_4R and related 5-$HT_{1A}R$, 5-$HT_{2A}R$ and α_1R were determined in competition binding experiments. Our initial observations were directed towards the identification of the optimal attachment point of the butoxy-linker and the positioning of potential functional groups at the pyrazolo[1,5-*a*]pyridine appendage. When the two

unsubstituted pyrazolo[1,5-*a*]pyridines **12a** and **12b** with the 2-methoxyphenylpiperazine head group were compared, the 6-butoxy analog **12a** showed superior binding properties towards all D_2-like receptor subtypes (K_i 0.69-5.0 nM compared to 13-18 nM for **12b**). Introduction of an ethyl carboxylate-, hydroxymethyl- or formyl-substituent into position 2 of the 5-butoxypyrazolo[1,5-*a*]pyridine moiety led to an approximately two fold improvement of $D_{2L}R$, $D_{2S}R$ and D_3R affinities for test compounds **12c-e** (K_i 5.1-8.1 nM, 5.5-7.4 nM, 7.4-15 nM at $D_{2L}R$, $D_{2S}R$ and D_3R, respectively) compared to the unsubstituted precursor **12b**. Interestingly, no significant differences in the D_4R affinity of test compounds **12b-e** were observed. Conversion into the oxime **12f** also slightly improved D_2R, D_3R and D_4R affinity (K_i 3.3, 1.9, 3.2 and 7.8 nM at $D_{2L}R$, $D_{2S}R$, D_3R and D_4R), indicating a beneficial effect of position-2 substituents on D_2/D_3 receptor affinity. In contrast, introduction of the linear and small cyano-group (**12g**) did not significantly alter the binding affinity for D_2R/D_3R compared to **12b**. However, none of the position 2 modifications could achieve the subnanomolar D_2R binding affinity of the unsubstituted 6-butoxypyrazolo[1,5-*a*]pyridine **12a**. In comparison to modifications at position 2 of the pyrazolo[1,5-*a*]pyridine moiety, we investigated the effects of similar substituents in position 3 of the aromatic heterocycle, since this position had previously been identified as suitable attachment point for different functional groups.[10, 23] Interestingly, the introduction of these substituents had opposite effects within the group of 2-methoxyphenylpiperazines. While the introduction of a formyl residue led to an improvement of the D_2R affinity for the 5-butoxy-derivative **14b**, D_2R affinity was reduced for the 6-butoxy analog **14a** (K_i 1.8 and 2.3 nM at $D_{2S}R$ and $D_{2L}R$ for **14b** vs. 7.8 and 7.7 nM for **14a**). The same trend was also observed for the oxime-substituted analogs **16a** (6-butoxy, K_i 4.2 and 1.7 for $D_{2L}R/D_{2S}R$) compared to **16b**/**c**. Especially, the (*E*) and *s-cis* configured isomer **16c** showed ultra-high affinity for $D_{2L}R$ and $D_{2S}R$ (K_i 0.16 and 0.094 nM). Sub-nanomolar binding affinity at $D_{2L}R$ /$D_{2S}R$ was also observed for the 3-cyano-derivative **18** (K_i 0.25 and 0.16 nM). In contrast to the set of 2-methoxyphenylpiperazines, substitution patterns of the

pyrazolo[1,5-*a*]pyridine appendage had only marginal influence on the affinity of compounds within the series of 5-aminotetraline head groups. Compared to the unsubstituted parent compounds (*S*)-**13a**/**b**, introduction of formyl or oxime moieties 3 did not alter D_2R affinities more than two-fold. In general, low nanomolar to subnanomolar affinities for D_2R/D_3R were observed within the entire compound family. More importantly, the absolute stereochemistry of the 5-hydroxy-*N*-propyl-2-aminotetraline was found to be responsible for the super-affinity, when the (*S*)-isomers **13a**/**b** were identified as eutomers with a 45- to 190-fold higher D_2R and 15-fold higher D_3R affinity compared to the (*R*)-enantiomers (K_i 0.63-2.1 nM and 0.71-0.80 nM at D_2R and D_3R for (*S*)-**13a**/**b** compared to 39-120 nM and 11-13 nM for (*R*)-**13a**/**b**). All compounds showed weak binding to the D_1R subtype (K_i 210-8600 nM). Noteworthy, the α_1 adrenoceptor affinity was found to be strongly correlated to the nature of the orthosteric head group. While all target compounds comprising a 2-methoxyphenylpiperazine moiety had binding affinities in the subnanomolar or low nanomolar range (K_i 0.32-7.2 nM), the α_1R affinity of ligands with a 5-hydroxy-*N*-propyl-2-aminotetraline unit was at least 100-fold lower (K_i 77-360 nM). Although not as pronounced, a similar trend was observed at serotonergic 5-$HT_{2A}R$, when aminotetralines displayed 2-to 10-fold lower affinities than 2-methoxyphenylpiperazines (K_i 880-2300 nM and 78-1500 nM). All compounds also displayed high to moderate affinity for 5-$HT_{1A}R$ (K_i 0.087-25 nM).

Table 2. Binding affinities of pyrazolo[1,5-*a*]pyridines **12a-g** to **18**.

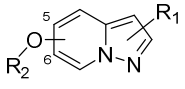

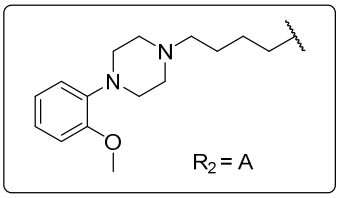

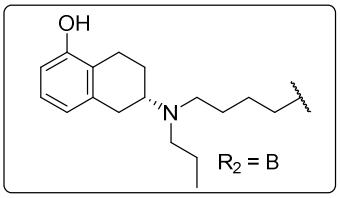

	R_1	R_2	K_i [nM]							
			hD_1[‡]	hD_{2L}[§]	hD_{2S}[§]	hD_3[§]	hD_4[§]	p5-HT_{1A}[††]	h5-HT_{2A}[‡‡]	pα_1[§§]
12a	H	6-A	1100 ± 260	1.8 ± 0.63	0.74 ± 0.16	5.0 ± 2.0	0.69 ± 0.032	3.3 ± 0.6	210 ± 13	1.3 ± 0.0
12b	H	5-A	2800 ± 850	18 ± 2.8	14 ± 2.1	20 ± 1.4	13 ± 0.71	3.0 ± 1.4	1100 ± 420	3.4 ± 0.92
12c	2-COOEt	5-A	410 ± 64	8.1 ± 5.4	7.4 ± 1.8	7.4 ± 2.2	11 ± 2.6	1.8 ± 0.67	78 ± 12	2.2 ± 0.14
12d	2-CH_2OH	5-A	920 ±540	6.0 ± 2.7	5.8 ± 3.7	15 ± 6.7	21 ± 7.0	0.68 ± 0.41	250 ± 28	1.6 ± 0.50
12e	2-CHO	5-A	470 ± 300	5.1 ± 2.0	5.5 ± 3.0	7.4 ± 1.1	19 ± 3.1	1.0 ± 0.40	180 ± 42	1.8 ± 0.28
12f	2-oxime	5-A	440 ± 85	3.3 ± 2.5	1.9 ± 1.0	3.2 ± 1.9	7.8 ± 4.5	0.41 ± 0.13	94 ± 29	7.2 ± 7.0
12g	2-CN	5-A	280 ± 7.1	12 ± 4.6	12 ± 3.5	12 ± 5.6	5.2 ± 2.5	0.60 ± 0.28	410 ± 210	3.9 ± 1.2
(*S*)-**13a**	H	6-B	2100 ± 570	0.63 ± 0.24	0.75 ± 0.12	0.71 ± 0.41	1.5 ± 1.1	5.3 ± 2.5	2000 ± 1000	360 ± 130
(*R*)-**13a**	H	6-B	8600 ± 4500	120 ± 39	48 ± 23	11 ± 5.7	54 ± 24	25 ± 8.5	1100 ± 320	160 ± 14
(*S*)-**13b**	H	5-B	800 ± 430	2.1 ± 0.29	0.70 ± 0.28	0.80 ± 0.27	1.2 ± 0.28	7.7 ± 0.78	1200 ± 70	96 ± 5.7
(*R*)-**13b**	H	5-B	3700 ± 3500	96 ± 30	39 ± 17	13 ± 1.7	84 ± 39	9.1 ± 1.3	1600 ± 71	310 ± 71
14a	3-CHO	6-A	1400 ± 71	7.8 ± 5.1	7.7 ± 2.8	17 ± 14	4.3 ± 0.92	0.59 ± 0.3	1500 ± 160	1.3 ± 0.77
14b	3-CHO	5-A	430 ± 240	1.8 ± 0.67	2.3 ± 1.4	12 ± 5.0	7.1 ± 2.5	1.1 ± 0.29	350 ± 85	1.1 ± 0.23
(*S*)-**15a**	CHO	6-B	1400 ± 350	2.4 ± 0.89	0.94 ± 0.19	1.6 ± 0.87	7.9 ± 4.5	6.6 ± 3.3	2300 ± 280	120 ± 14
(*S*)-**15b**	CHO	5-B	1300 ±350	2.3 ± 0.19	0.90 ± 0.21	1.1 ± 0.71	2.2 ± 0.71	1.6 ± 0.71	2200 ± 350	150 ± 42
16a	3-oxime	6-A	1000 ± 680	4.2 ± 2.5	1.7 ± 0.34	2.3 ± 0.78	4.7 ± 0.96	0.087 ± 0.054	100 ± 28	1.2 ± 0.40
16b	3-oxime (*E*)-*s-trans*	5-A	710 ± 28	1.2 ± 0.27	0.72 ± 0.32	4.5 ± 2.2	1.5 ± 0.28	6.2 ± 0.21	91 ± 13	0.70 ± 0.01
16c	3-oxime *(E)-s-cis*	5-A	860 ± 78	0.16 ± 0.02	0.094 ± 0.027	3.3 ± 1.2	0.73 ± 0.12	6.6 ± 2.1	100 ± 23	0.62 ± 0.18
(*S*)-**17a**	3-oxime	6-B	600 ± 160	2.5 ± 1.1	0.84 ± 0.28	0.41 ± 0.18	6.5 ± 4.8	5.0 ± 1.9	880 ± 360	77 ± 26

(*S*)-**17b**	3-oxime	5-B	1800 ± 500	2.2 ± 0.52	0.87 ± 0.20	0.59 ± 0.03	2.0 ± 0.28	3.0 ± 1.5	1600 ± 640	140 ± 7.1
18	3-CN	5-A	210 ± 57	0.25 ± 0.12	0.16 ± 0.02	2.9 ±2.4	1.3 ± 1.2	1.0 ±0.0	110 ± 44	0.32 ± 0.04

[†]Data represent mean ± S.D. of two to fifteen independent experiments, each performed in triplicate. Radioligands: [‡][^{3}H]SCH23990, [§][^{3}H]spiperone, [††][^{3}H]WAY100635, [‡‡][^{3}H]ketanserin, [§§][^{3}H]prazosin.

Activation of G proteins. The influence of the different attachment points of the 2-methoxyphenylpiperazine via the butoxy-spacer (position 5 or 6 of the heterocycle) and varying polar substituents of the pyrazolo[1,5-*a*]pyridine moiety on $D_{2S}R$ and D_3R activation was investigated in [^{35}S]GTPγS binding experiments (Table 3). In addition to studying $D_{2S}R$ and D_3R mediated nucleotide exchange with $G\alpha_{oA}$, we also investigated the $D_{2S}R$ promoted activation of the widely expressed $G\alpha_{i2}$ subunit,[34] since D_2R is known to promiscuously couple to the $G\alpha_{i/o}$ family.[31] In all three test systems, 2-methoxyphenylpiperazines were found to activate the receptors with submaximal efficacy, indicating partial agonists profiles similar to the antipsychotic **1a**. However, differences in the relative potencies and efficacies were detected in a careful data analysis. Compared to **1a**, the two unsubstituted pyrazolo[1,5-*a*]pyridines **12a** and **12b** showed lower efficacies for the activation of $D_{2S}R$. Whereas **12b** displayed potencies similar to **1a**, **12a** with the butoxy-spacer in position 6 of the heterocycle was about ten-fold more potent for the activation of $D_{2S}R$. At the D_3R differences in potencies were less pronounced but **1a** was less effective than the two target compounds (Supplementary Figures 1a, 3a,b). Introduction of a formyl residue into position 3 of the pyrazolo[1,5-*a*]pyridine heterocycle preserved the activation properties in the case of the 6-butoxy derivative **14a** (EC_{50} 5.9, 150 nM, and 19 nM, E_{max} 38 %, 25 % and 71 % at $D_{2S}R/G\alpha_{oA}$, $D_{2S}R/G\alpha_{i2}$ and $D_3R/G\alpha_{oA}$). The same modification led to an increase in potency and intrinsic activity for $D_{2S}R/G\alpha_{oA}$ activation for the 5-butoxy analog **14b** (EC_{50} 17 nM, E_{max} 58 %), compared to its precursor **12b** (Supplementary Figure 3a,b and 3j,k). Interestingly, the efficacy was reduced by a factor of two for $D_{2S}R/G\alpha_{i2}$, leading to a substantial preference for $G\alpha_{oA}$ over $G\alpha_{i2}$ activation at $D_{2S}R$ for the 3-carbaldehyde **14b**. In agreement with their high binding affinities, the corresponding oximes **16a-c** also showed highly potent receptor

activation characteristics. Oxime **16a** with a 6-butoxy spacer showed a relative preference for $D_3R/G\alpha_{oA}$ activation (Supplementary Figure 3m), while the different stereoisomers with the 5-butoxy-spacer **16b**,**c** preferentially activated $G\alpha_{oA}$ proteins via $D_{2S}R$ (EC_{50} 3.4 and 0.74 nM for $D_{2S}R/G\alpha_{oA}$ vs. 41 nM and 18 nM for $D_3R/G\alpha_{oA}$ Supplementary Figure 3n,o).

Table 3. Functional properties of pyrazolo[1,5-*a*]pyridines **12a-g** to **14a,b** and **16a-c** and **18** compared to the reference **1a**, determined by [^{35}S]GTPγS binding.

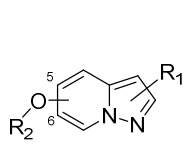

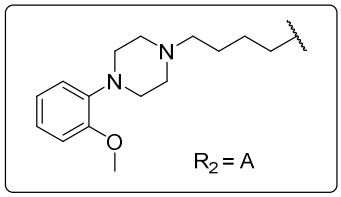

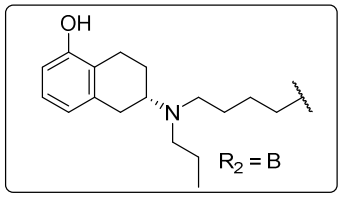

			[^{35}S]GTPγS binding†								
			$D_{2S}G\alpha_{oA}$			$D_{2S}G\alpha_{i2}$			$D_3G\alpha_{oA}$		
	R_1	R_2	pEC_{50}	EC_{50}‡	E_{max}§	pEC_{50}	EC_{50}‡	E_{max}§	pEC_{50}	EC_{50}‡	E_{max}§
1a	-	-	7.41 ± 0.09	39	67 ±2	6.80 ± 0.20	160	29 ± 3	7.71 ± 0.17	20	52 ± 3
12a	H	6-A	8.39 ± 0.15	4.1	30 ± 1	7.64 ± 0.21	23	25 ± 2	7.54 ± 0.08	29	62 ± 2
12b	H	5-A	7.38 ± 0.05	42	48 ± 1	6.73 ± 0.12	190	31 ± 2	7.25 ± 0.16	56	79 ± 5
12c	2-COOEt	5-A	6.72 ± 0.15	190	37 ± 3	6.16 ± 0.15	690	28 ± 3	7.30 ± 0.15	50	63 ± 3
12d	2-CH_2OH	5-A	7.14 ± 0.15	73	47 ± 3	6.02 ± 0.13	960	39 ± 3	7.57 ± 0.19	27	65 ± 5
12e	2-CHO	5-A	7.06 ± 0.12	88	46 ± 2	5.52 ± 0.19	2900	31 ± 6	8.02 ± 0.20	9.7	54 ± 4
12f	2-oxime	5-A	6.40 ± 0.12	400	35 ± 2	5.97 ± 0.17	1100	31 ± 4	7.16 ± 0.17	70	52 ± 3
12g	2-CN	5-A	5.85 ± 0.10	1400	42 ± 3	6.00 ± 0.21	980	29 ± 4	7.51 ± 0.22	31	48 ± 4
(*S*)-**13a**	H	6-B	8.69 ± 0.05	2.0	95 ± 2	7.59 ± 0.06	26	92 ± 2	9.32 ± 0.12	0.48	92 ± 4
(*S*)-**13b**	H	5-B	8.31 ± 0.04	4.9	102 ± 2	7.26 ± 0.06	55	98 ± 2	9.37 ± 0.10	0.43	104 ± 3
14a	3-CHO	6-A	8.23 ± 0.09	5.9	38 ± 1	6.81 ± 0.26	150	25 ± 3	7.73 ± 0.07	19	71 ± 2
14b	3-CHO	5-A	7.76 ± 0.11	17	58 ± 3	7.80 ± 0.34	16	17 ± 2	8.11 ± 0.16	7.7	54 ± 3
16a	3-oxime	6-A	8.54 ± 0.06	2.9	57 ± 1	9.36 ± 0.46	0.44	14 ± 2	9.49 ± 0.09	0.32	58 ± 2
16b	3-oxime *(E)-s-trans*	5-A	8.47 ± 0.09	3.4	47 ± 1	6.56 ± 0.17	270	25 ± 2	7.39 ± 0.14	41	74 ± 4
16c	3-oxime *(E)-s-cis*	5-A	9.13 ± 0.09	0.74	50 ± 1	6.93 ± 0.15	120	21 ± 2	7.74 ± 0.10	18	76 ± 3
18	3-CN	5-A	7.89 ± 0.12	13	47 ± 2	6.60 ± 0.27	250	22 ± 3	7.72 ± 0.19	19	75 ± 6

†Data represent mean ± S.E.M. from the pooled curve of four to ten independent experiments, each performed in triplicate. ‡Potency given in nM. §Efficacy normalized to the reference agonist quinpirole (100%) and buffer (0%).

In contrast to the beneficial effects of substituents in position 3 of the pyrazolo[1,5-*a*]pyridine heterocyle, the same functional groups did not have a positive impact on D_2R activation when they were attached to position 2 (Supplementary Figure 3c-g). On the contrary, compounds **12c-g** display lower potencies for promoting nucleotide exchange in membrane preparations from HEK293T cells expressing $D_{2S}R$ together with $G\alpha_{oA}$ or $G\alpha_{i2}$ (EC_{50} 73-1400 nM and E_{max} 35-47% for $G\alpha_{oA}$; EC_{50} 690-2900 nM and E_{max} 28-39% for $G\alpha_{i2}$) compared to the unsubstituted congener **12b** (42 nM, 48% for $G\alpha_{oA}$ and 190 nM, 31% for $G\alpha_{i2}$). At the same time, introduction of substituents had only a marginal influence on the potency observed for the activation of D_3R (EC_{50} 9.7-70 nM vs. 56 nM), while efficacies (E_{max} 52-65 %) were slightly decreased relative to **12b** (E_{max} 79 %). Compared to the partial agonist profiles observed for 2-methoxyphenylpiperazines, two representative pyrazolo[1,5-*a*]pyridines with an aminotetraline head group ((*S*)-**13a**,**b**) displayed full agonist characteristics for the three investigated systems ($D_{2S}R$ + $G\alpha_{oA}$, $D_{2S}R$ + $G\alpha_{i2}$, and D_3R + $G\alpha_{oA}$, Supplementary Figure 3h,i). Both compounds showed similar low to subnanomolar potencies and the same rank order with the highest potency for the activation of $D_3R/G\alpha_{oA}$ (EC_{50} 0.48 and 0.43 nM) followed by $D_{2S}R/G\alpha_{oA}$ (EC_{50} 2.0 and 4.9 nM) and finally $D_{2S}R/G\alpha_{i2}$ (EC_{50} 26 and 55 nM).

Further functional characterization. Although measurements of nucleotide exchange in form of [^{35}S]GTPγS binding experiments represent a direct method to assess receptor-mediated activation of G proteins without the amplification of a second messenger pathways, they also have their limitations.[35, 36] For instance, the different Gα isoforms vary in the nucleotide exchange rates, leading to diverse but generally low signal to background ratios, which in turn may require experiments to be carried out under different conditions.[35, 37] Very recently, it has been demonstrated that assay kinetics also play an important role when ligand bias or functional selectivity is examined, as it may lead to an observational bias.[38] In order to overcome these issues, we employed recently developed bioluminescence resonance

energy transfer (BRET) test system for the activation of G proteins.[39-42] Based on resonance energy transfer between *Renilla* Luciferase (RLucII) tagged-Gα and GFP10-Gγ$_2$ and hence the separation of Gβγ from Gα subunits, these highly sensitive systems allow a rapid investigation of receptor-mediated G protein activation under highly similar conditions for a broad variety of G proteins and different receptors.[39-42]

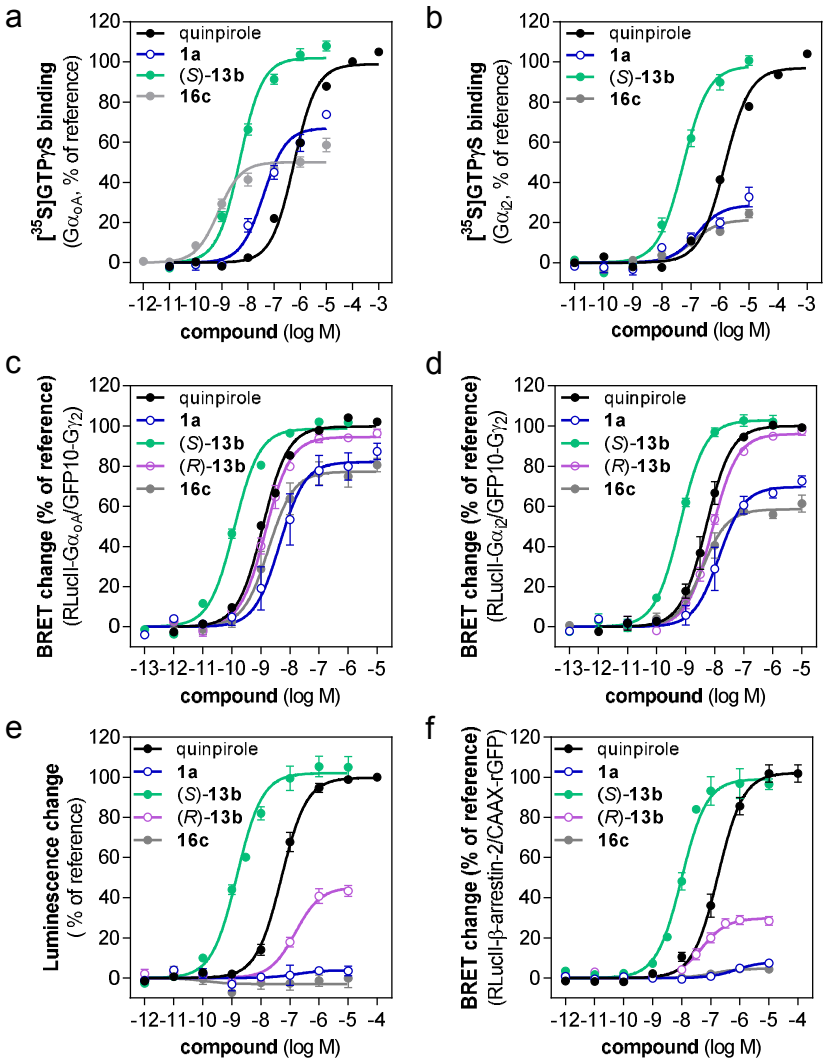

Figure 3. Functional properties of pyrazolo[1,5-*a*]pyridines **16c**, (*S*)-**13b** and (*R*)-**13b** in comparison to the full agonist quinpirole and the reference antipsychotic **1a** at $D_{2S}R$. Activation of $G\alpha_{oA}$ (**a**,**c**) and $G\alpha_{i2}$ (**b**,**d**) was determined either by [^{35}S]GTPγS binding (**a**,**b**) or by BRET changes occurring upon separation of RLucII-$G\alpha_{i/o}$ from GFP10-Gγ$_2$ (**c**,**d**). Ligand-stimulated recruitment of β-arrestin-2 was determined employing the PathHunter assay (**e**) or an approach based on bystander BRET (**f**). Data wase normalized relative to the response of quinpirole (100 %) and vehicle (0 %) and represent mean ± S.E.M. from three to ten independent experiments, each performed at least in duplicate.

A series of BRET titration experiments was performed to confirm coupling of the different $G\alpha_{i/o}$ biosensors with $D_{2S}R$, $D_{2L}R$ and D_3R. $D_{2S}R$ and $D_{2L}R$ gave robust BRET

changes upon stimulation with the endogenous agonist dopamine for both $G_{\alpha i1\text{-}3}$ and $G\alpha_{oA/B}$ (Supplementary Figure 4a-j), which coincides with earlier reports on promiscuous coupling of D_2R to the entire family $G\alpha_{i/o}$ proteins.[31] Robust BRET changes upon dopamine treatment indicated a preferential interaction with $G\alpha_{oA/B}$ for D_3R,[30] while only small BRET changes were observed with $G_{\alpha i1\text{-}3}$, suggesting a minor interaction of D_3R with these subunits (Supplementary Figure 4k-o). From these titrations, optimal transfection conditions were derived for the individual biosensors to obtain dose-response curves for a subset of the newly synthesized ligands and the five $G\alpha_{i/o}$ subunits in coexpression with $D_{2S}R$ (Table 4, Supplementary Figure 5a-p) and $D_{2L}R$ and the two $G\alpha_o$ isoforms for D_3R (Supplementary Table 1). In all investigated systems, the two reference agonists quinpirole and dopamine showed a highly similar behavior (Supplementary Figure 5a,b). In general, only small differences were observed among the three $G\alpha_i$ or two $G\alpha_o$ isoforms although potencies were found to be slightly better (2-5 fold) for the activation of the $G\alpha_o$ proteins. However, dopamine was a little less effective in activating the $G\alpha_o$ pathways (E_{max} 87-92 %), which is in good agreement with the results from [^{35}S]GTPγS binding experiments. Results obtained with $D_{2L}R$ showed no significant differences to those obtained with the short isoform $D_{2S}R$. All compounds sharing an (*S*)-aminotetraline moiety were found to be highly potent agonists (EC_{50} 0.11-0.96 nM) for the $D_{2S}R$-mediated activation of the different $G\alpha_{i/o}$ isoforms. In agreement with the reduced binding affinities, enantiomers (*R*)-**13a**/**b** were 10- to 20-fold less potent (EC_{50} 1.5-9.8 nM), while retaining full agonist efficacies (Supplementary Figure 5e-h,k,l,o,p). On the contrary, all ligands bearing a 2-methoxyphenylpiperazine pharmacophore shared partial agonist properties for the activation of all $G\alpha_{i/o}$ proteins. Although efficacies were generally found to be higher when compared to the results from [^{35}S]GTPγS binding, the preferential activation of $G\alpha_o$ over $G\alpha_i$ was preserved in the BRET readings. Both, efficacies and potencies were found to be higher for the activation of $G\alpha_{oA/B}$, (E_{max} 77-86 % vs. 39-62 % and EC_{50} 1.5-4.3 nM vs. 2.1-13.1 nM for $G\alpha_{oA/B}$ vs. $G\alpha_{i1\text{-}3}$) indicating a functionally selective

D_2R activation mode for the investigated 1,4-DAPs. Importantly, when compared to the approved antipsychotic **1a**, 1,4-DAPs comprising a pyrazolo[1,5-*a*]pyridine appendage, were found to show similar activation profiles with higher overall potency (Figure 3a-d).

Recruitment of β-arrestins. In addition to the investigations of canonical G protein signaling, we determined the ligands' ability to induce β-arrestin-2 recruitment upon binding to $D_{2S}R$ employing the PathHunter assay, as previously described.[10, 23] Experiments unambiguously showed the impact of the orthosteric head group on the intrinsic activity (Table 4, Figure 3e,f). Similar to the reference antipsychotic **1a**, the investigated 2-methoxyphenylpiperazines displayed antagonist, or at most weak partial agonist properties with a maximum effect less than 10 % of the reference agonist quinpirole at $D_{2S}R$ (Table 4, Supplementary Figure 2b). In contrast, all compounds sharing a (*S*)-5-hydroxy-2-aminotetraline head group were found to be potent agonists. Observed maximum effects (E_{max} 93-105 %) were comparable to the reference agonist quinpirole or dopamine and in agreement with their superior binding affinities and potencies to activate G proteins, ligands (*S*)-**13a**,**b**, (*S*)-**15a**,**b** and (*S*)-**17a**,**b** were found to be up to 120-fold more potent (EC_{50} 1.3-3.0 nM) than the endogenous agonist. Similar to the above described results, addition of functional groups to the pyrazolo[1,5-*a*]pyridine appendage did not significantly influence β-arrestin-2 recruitment for ligands with an 5-hydroxy-2-aminotetraline head group. Importantly, inversion of the stereogenic center into its (*R*)-configuration converted the potent agonists into partial agonists with only moderate potencies (E_{max} 49-51%, EC_{50} 161-218 nM). Since the same compounds were found to fully activate the panel of $G\alpha_{i/o}$ proteins, the inversion of the stereogenic center converted the two balanced agonists (*S*)-**13a**,**b** into G-protein-biased ligands ((*R*)-**13a**,**b**). The apparent preference for G protein mediated-signaling of (*R*)-**13a,b** was further confirmed by a quantitative analysis of ligand bias using the operational model of agonism.[43-45] As representative pathways, we selected the activation of $G\alpha_{oA}$ as G protein readout and compared it to the recruitment of β-arrestin-2 determined in the PathHunter assay.

While (*S*)-**13a/b** showed only small differences from the reference ligand quinpirole with a slight preference for the arrestin signaling ($\Delta\Delta\log(\tau/K_A)$ = -0.25 and -0.46, Supplementary Table 2) the respective (*R*)-enantiomers displayed an almost 10-fold preference for the canonical signaling pathway ($\Delta\Delta\log(\tau/K_A)$ = 0.96 and 0.88, bias factors 9.09 and 7.65 for (*R*)-**13a** and (*R*)-**13b** respectively). Interestingly, the quantification also a revealed a preferential activation of β-arrestin-2 signaling the oxime-substituted analogs (*S*)-**17a,b** ($\Delta\Delta\log(\tau/K_A)$ = -0.65 and -0.58) which was statistically significant but not obvious from the visual analysis. Since the operational model is not feasible for the analysis of very weak partial agonists or antagonists,[46] ligand bias between $G\alpha_{oA}$ activation and β-arrestin-2 recruitment could not be quantified for the family of 1,4-DAPs.

Considering the importance of cell background, kinetics and experimental conditions in the context of putative ligand bias,[38, 47] we intended to complement our β-arrestin recruitment studies by an orthogonal BRET assay. Thus, we employed a recently described approach, which is based on enhanced bystander BRET between RLucII-β-arrestin-1 or β-arrestin-2 and the CAAX-motif of KRas C-terminally fused to *Renilla reniformis* green fluorescent protein (rGFP).[48] This system allowed to asses G protein activation and β-arrestin recruitment on the same time scale (within minutes) and in the same cell background (HEK293). We also coexpressed G protein-coupled receptor kinase 2 (GRK2), as it has been shown to enhance ligand-induced β-arrestin recruitment, especially for D_2R partial agonists.[12] Using this setup, highly similar results were obtained for pyrazolo[1,5-*a*]pyridine-derived test compounds. Indeed, the propensity to induce β-arrestin recruitment at $D_{2S}R$ (Table 4) or $D_{2L}R$ (Supplementary Table 1) was confirmed to depend on the orthosteric head group. While (*S*)-aminotetralines acted as full agonists (E_{max} 83-100 %, EC_{50} 10.5-17.7 nM), their (*R*)-enantiomers showed moderate partial agonist characteristics (E_{max} 26-31 %, EC_{50} 48-98 nM) for the two β-arrestin isoforms. Again no significant β-arrestin recruitment was observed for ligands containing a 2-methoxyphenylpiperazine pharmacophore. These antagonist properties

were further confirmed by inhibition experiments with both, the PathHunter and BRET-based assays, when the ligands were able to inhibit the effect of 0.1 μM or 1 μM quinpirole, respectively (Supplementary Figure 6a-d).

Table 4. Functional properties of selected pyrazolo[1,5-*a*]pyridines compared to the reference **1a**, for the activation of the five different $G\alpha_{i/o}$ subunits $D_{2S}R$ and β-arrestin recruitment, determined by BRET or the PathHunter assay.

	$D_{2S}R$ activation[†]															
	BRET														PathHunter	
	$G\alpha_{i1}$		$G\alpha_{i2}$		$G\alpha_{i3}$		$G\alpha_{oA}$		$G\alpha_{oB}$		β-arr1		β-arr2		β-arr2	
	EC_{50}[‡]	E_{max}[§]	EC_{50}[‡]	E_{max}[§]	EC_{50}[‡]	E_{max}[§]	EC_{50}[‡]	E_{max}[§]	EC_{50}[‡]	E_{max}[§]	EC_{50}[‡]	E_{max}[§]	EC_{50}[‡]	E_{max}[§]	EC_{50}[‡]	E_{max}[§]
quinpirole	3.0 ± 0.5	100 ± 1	5.1 ± 1.3	100 ± 1	5.9 ± 0.7	100 ± 1	1.2 ± 0.10	100 ± 1	1.2 ± 0.1	100 ±1	295 ± 100	100 ± 1	151 ± 10	100 ± 1	64 ± 8	100 ± 1
dopamine	2.8 ± 0.6	100 ± 6	3.9 ± 0.6	102 ± 3	4.5 ± 0.2	95 ± 3	0.67 ± 0.17	92 ± 3	0.78 ± 0.15	87 ±5	226 ± 53	115 ± 7	163 ± 35	113 ± 5	156 ± 36	92 ± 4
1a	14.9 ± 7.8	70 ± 2	19.4 ± 9.7	71 ± 2	17.5 ± 7.5	62 ± 1	8.7 ± 4.2	81 ± 6	4.8 ± 1.9	82 ±5	n.d.[††]	< 15	n.d.[††]	< 10	n.d.[††]	<10
12a	2.1 ± 0.2	53 ± 5	4.4 ± 0.5	47 ± 6	5.0 ± 0.2	39 ± 5	1.5 ± 0.10	81 ±2	1.9 ± 0.2	81 ±3	n.d.[††]	< 10	n.d.[††]	< 10	n.d.[††]	< 10
(*S*)-**13a**	0.30 ± 0.02	95 ± 1	0.61 ± 0.05	102 ± 1	0.81 ± 0.05	102 ± 2	0.13 ± 0.01	98 ± 1	0.11 ± 0.01	99 ± 2	13.7 ± 2.8	95 ± 2	15.9 ± 1.3	100 ± 4	3.0 ± 0.4	93 ± 5
(*R*)-**13a**	5.5 ± 0.2	93 ± 1	8.7 ± 0.8	93 ± 2	9.6 ± 0.7	83 ± 2	1.7 ± 0.4	98 ± 3	2.2 ± 0.4	100 ± 2	98 ± 40	31 ± 4	61 ± 20	26 ± 1	218 ± 33	51 ± 3
(*S*)-**13b**	0.30 ± 0.01	97 ± 1	0.65 ± 0.03	103 ± 3	0.80 ± 0.18	101 ± 1	0.12 ± 0.01	99 ± 1	0.12 ± 0.01	102 ± 1	14.5 ± 3.0	100 ± 4	10.5 ± 1.0	99 ± 5	1.3 ± 0.1	97 ± 5
(*R*)-**13b**	5.2 ± 0.7	101 ± 3	8.4 ± 0.8	96 ± 1	9.8 ± 1.2	88 ± 2	1.5 ± 0.3	95 ± 1	1.7 ± 0.1	100 ± 2	48 ± 3.0	31 ± 4	54 ± 22	27 ± 3	161 ± 22	49 ± 3
14a	4.2 ± 0.2	61 ± 1	7.7 ± 1.2	54 ± 3	10.1 ± 0.78	47 ± 3	2.6 ± 0.6	84 ± 1	2.6 ± 0.2	82 ± 2	n.d.[††]	< 10	n.d.[††]	< 10	n.d.[††]	< 10
(*S*)-**15a**	0.31 ± 0.04	97 ± 1	0.54 ± 0.18	100 ± 1	0.72 ± 0.12	99 ± 1	0.13 ± 0.02	99 ± 1	0.12 ± 0.02	100 ± 1	17.7 ± 5.5	95 ± 6	13.4 ± 1.2	96 ± 2	3.0 ± 0.9	97 ± 4
(*S*)-**15b**	0.39 ± 0.05	103 ± 1	0.71 ± 0.12	106 ± 1	0.74 ± 0.02	102 ± 2	0.11 ± 0.01	99 ± 1	0.11 ± 0.01	100 ± 1	12.5 ± 1.6	99 ± 3	12.4 ± 1.5	91 ± 6	2.9 ± 0.8	96 ± 4
16a	6.8 ± 0.7	59 ± 5	10.7 ± 0.3	53 ± 5	13.1 ± 2.8	45 ± 4	2.9 ± 0.8	82 ±2	4.3 ± 0.4	86 ± 2	n.d.[††]	< 10	n.d.[††]	< 10	n.d.[††]	< 10
16b	3.7 ± 0.9	59 ± 6	5.7 ± 0.2	56 ± 8	5.7 ± 0.8	43 ± 5	1.8 ± 0.4	86 ±1	2.1 ± 0.2	84 ± 1	n.d.[††]	< 10	n.d.[††]	< 10	n.d.[††]	< 10
16c	5.0 ± 2.2	62 ± 3	5.8 ± 2.2	59 ± 2	6.2 ± 2.4	50 ± 2	2.5 ± 0.7	77 ± 5	2.0 ± 0.7	82 ± 4	n.d.[††]	< 15	n.d.[††]	< 10	n.d.[††]	< 10
(*S*)-**17a**	0.39 ± 0.09	99 ± 4	0.60 ± 0.02	103 ± 3	0.94 ± 0.12	99 ± 2	0.19 ± 0.02	99 ± 1	0.16 ± 0.01	103 ± 1	13.1 ± 1.3	92 ± 6	12.1 ± 1.3	96 ± 5	1.5 ± 0.2	99 ± 4
(*S*)-**17b**	0.49 ± 0.08	99 ± 1	0.67 ± 0.08	101 ±1	0.96 ± 0.14	98 ±1	0.21 ± 0.04	101 ±2	0.17 ± 0.03	101 ± 1	11.9 ± 1.6	83 ±2	13.2 ± 2.2	92 ±2	1.7 ± 0.4	105 ± 6

[†]Data represent mean ± S.E.M. from three to six independent experiments, each performed in duplicates. [‡]EC_{50} given in nM. [§]E_{max} relative to the effect of vehicle (0 %) and the saturating effect of quinpirole (100 %). [††]Not determined.

Activation of inwardly rectifying potassium channels. In addition to the measurements of nucleotide exchange or resonance energy transfer at the G protein level, we examined the intrinsic activity of representative partial agonists further downstream at the level of G protein-coupled, inwardly rectifying potassium (GIRK) channels. GIRK-mediated signaling is involved in a number of important physiological processes, including nociception, reward-related behavior, cognition, mood and the regulation of the heart rate.[49] GIRK activation increases outward K^+-currents, leads to cellular hyperpolarization[50] and is therefore known as key inhibitory mediator for the control of electrical excitability.[51] Recently, a genome-wide association study revealed a link between the *KCNJ3*, the gene encoding GIRK1, and the susceptibility for schizophrenia and bipolar disorders in Asian populations.[52, 53] Furthermore, it has been demonstrated that lithium exerts its efficacy in bipolar disorders by a dual regulation of GIRKs.[54] Both, D_2R and D_3R have been shown to couple to GIRK channels *in vitro*.[55, 56] Interestingly, typical antipsychotics including haloperidol act as antagonists or even inverse agonists for D_2R mediated GIRK activation, while newer generation antipsychotics including **1a** have been described as antagonists or partial agonists.[57, 58] To compare the properties of the high affinity, high potency pyrazolo[1,5-*a*]pyridine **16c** with the marketed drug **1a** and the endogenous agonist dopamine, we performed voltage clamp experiments in analogy to a previously described procedure.[59] When HEK293T cells expressing either $D_{2L}R$ or D_3R together with GIRK1/2, the predominant GIRK heteromer in the CNS,[60] were stimulated with the endogenous agonist dopamine, robust K^+-currents were observed (Figure 4a). Current-voltage diagrams revealed typical inwardly rectifying profiles (Supplementary Figure 7a,b) and currents were efficiently blocked by application of Ba^{2+} or the D_2R/D_3R-antagonist haloperidol (Figure 4a, Supplementary Figure 7c,d). Currents were evoked in a $G\alpha_{i/o}$-specific manner, as overnight incubation with pertussis toxin completely abolished the dopamine-mediated effects (Supplementary Figure 7e,f). Although not to the same extent as dopamine, phenylpiperazines

1a and **16c** stimulated GIRK1/2 activation when they were applied at a concentration of 1 µM to cells expressing $D_{2L}R$ and GIRK1/2. Again, the effect was inhibited by application of the pore blocker Ba^{2+}. At lower concentration (0.1 µM) only **16c** but not **1a** induced a significant effect (Supplementary Figure 7g) pointing towards a higher potency of the pyrazolo[1,5-*a*]pyridine.

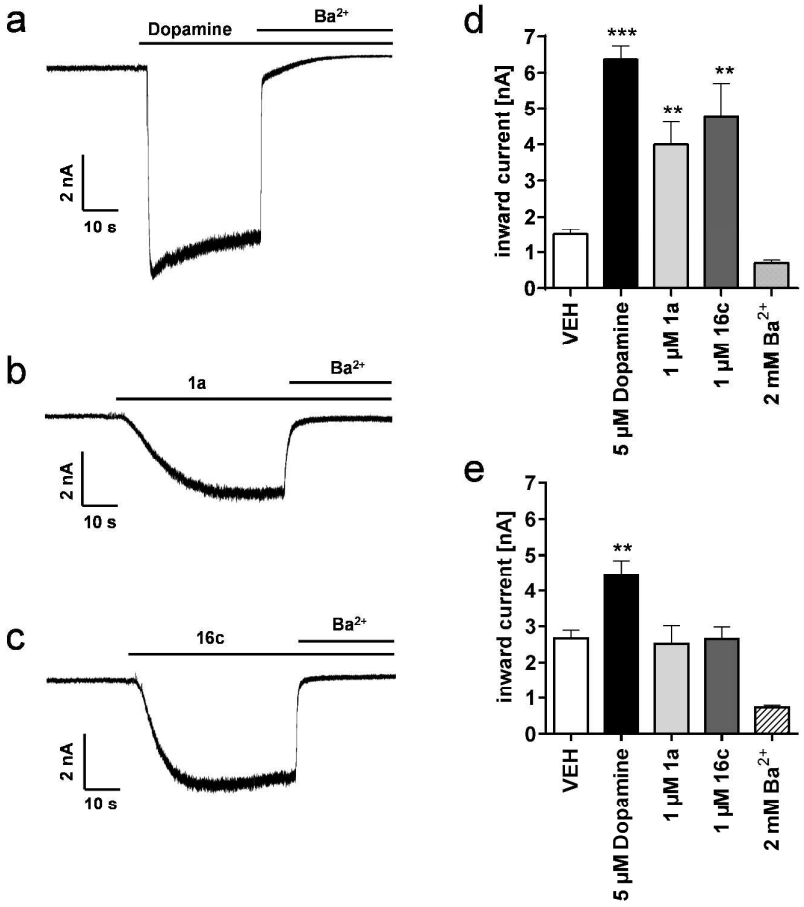

Figure 4. Ligand-induced activation of GIRK1/2 channels. When HEK293T cells expressing $D_{2L}R$ and GIRK1/2 cells were stimulated with 10 µM dopamine (**a**) 1 µM **1a** (**b**) or 1 µM **16c** (**c**), a robust K^+ current is induced at the holding potential of -70 mV in high K^+ external solution. Currents are completely inhibited by subsequent addition of a 2 mM $BaCl_2$ into the bath solution. Quantification of $D_{2L}R$ activation from ramp currents shows a partial response is elicited by **1a** and **16c** compared to the endogenous agonist dopamine (**d**). In HEK293T cells expressing D_3R and GIRK1/2 only dopamine, but not 1 µM solutions of **1a** or **16c** evoke a significant K^+ current (**e**). Data represent mean ± S.E.M. from 9 to 30 individual cells, VEH = vehicle, ** = $p < 0.01$, *** $p < 0.001$, one-way ANOVA.

In the absence of receptors, neither dopamine nor **1a** or **16c** elicited an increase in K^+-currents (Supplementary Figure 7h). In cells expressing the D_3R, no effect was observed for the partial agonists (Figure 4e), indicating a different capacity of the ligands to stimulate

GIRK1/2 by means of $D_{2L}R$ or D_3R. Moreover, differences in GIRK1/2 activation may reflect the distinctions observed in signaling signatures for $D_{2L}R$ and D_3R observed by BRET. While $D_{2L}R$ is capable to equally engage $G\alpha_i$ and $G\alpha_o$, D_3R shows a strong preference for the $G\alpha_o$ subtypes and only minor coupling to $G\alpha_{i1-3}$ (Supplementary Figure 4).

***In vivo* antipsychotic activity.** In order to examine if G protein-biased D_2R/D_3R partial agonists comprising a pyrazolo[1,5-*a*]pyridine appendage possess antipsychotic activity *in vivo*, we investigated the representative test compound **16c** in comparison to **1a**, regarding their effects on schizophrenia-related behaviors in rats. As readouts, we examined locomotion and anxiety, which have been used extensively in animal models of schizophrenia.[61-63] Additionally, we investigated light induced activity (LIA), a non-aversively motivated sensorimotor processing measure,[64, 65] to assess the intactness of the sensorimotor gating system.[64, 66] In order to induce schizophrenia-like alterations in animals, we used an amphetamine (AMPH)-sensitization regimen that has been developed by Peleg-Raibstein et al. and shown to effectively induce these disruptions.[62] Thus, after a six day sensitization with escalating doses of AMPH, antipsychotic **1a,** test compound **16c** (both at a dose of 1.5mg/kg/day) or vehicle were continuously administered via an osmotic Alzet mini pump over the course of seven days. LIA was measured on day five after mini pump implantation and behavioral testing in the open field (OF) environment was performed on treatment day seven before (baseline) and after an acute AMPH (1.5 mg/kg) challenge. Pre-planned comparisons revealed a decrement in the baseline locomotor activity in all treatment groups relative to the SAL/VEH control group (Figure 5a,b, Supplementary Results). Compared to this baseline activity, we found increased horizontal and vertical (rearing) locomotor responses to the low dose amphetamine-challenge in AMPH-sensitized animals, which has been frequently reported (for a review, see ref. [67]). These elevations were reversed by continuous treatment with both **1a** and **16c**. **16c** treatment was arguably more effective than **1a** treatment in inhibiting AMPH-induced hyper-locomotor activity (Figure 5d,g,e,h).

However, baseline activity was influenced by the treatments. Indeed, **16c** treatment inhibited the baseline locomotor activity as opposed to no alterations observed with **1a** (Figure 5a,b). Central activity in the OF test is a useful parameter to estimate the anxiety level of animals,[68] and several comorbid anxiety disorders have been associated with AMPH abusers[69] and schizophrenia patients.[70, 71] AMPH-pretreated animals showed elevated anxiety, as indicated by a decreased time spent in the center of the OF (Figure 5c). Treatment with **1a** or **16c** did not alter baseline anxiety levels. However, **16c** but not **1a**, at least partially reversed the effects of an acute amphetamine challenge (Figute 5f,i). Finally, AMPH-sensitization caused disruptions in sensorimotor gating, which was measured by light-induced activity test. These disruptions were partially improved by both **1a** and **16c** treatments (Supplementary Figure 8a,b). The results show that **16c** treatment effectively reverses amphetamine-induced hyper-locomotor activity in rats, but unlike **1a**, **16c** treatment exacerbates the baseline locomotion-related attenuations induced by AMPH-pretreatment. Extrapyramidal deficits are common side effects of many antipsychotic drugs, including both typical and atypical ones.[72, 73] Altogether, these results indicate that **16c** treatment can effectively improve schizophrenia-like disruptions *in vivo*, but as a side effect, may reduce general locomotor activity.

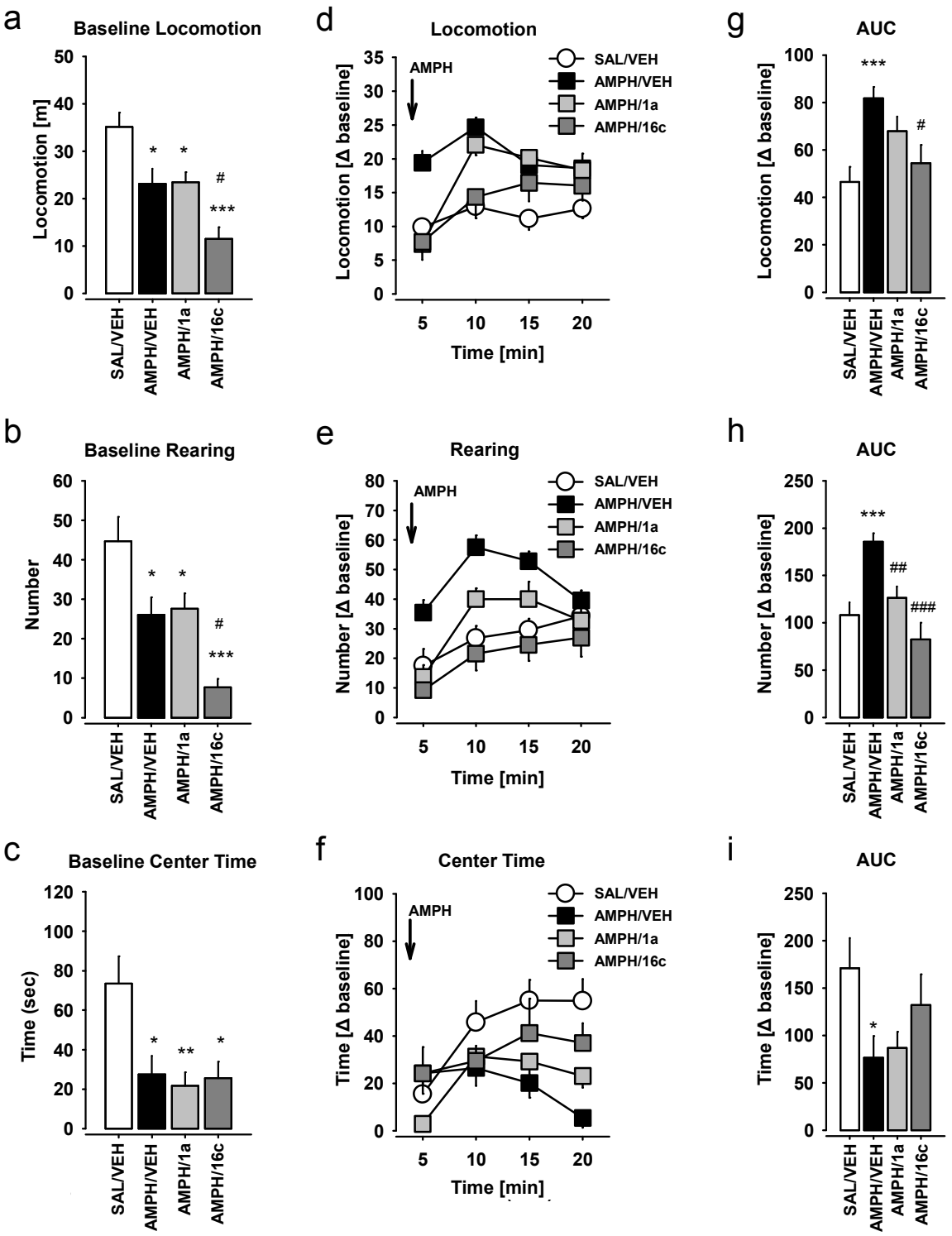

Figure 5. The effects of **16c** compared to **1a** on schizophrenia-like behavior in rats. Animals received i.p. injections of amphetamine (AMPH) with a sensitization regimen or saline (SAL). Subsequently, the animals were continuously treated with **1a** (1.5 mg/kg/day), **16c** (1.5 mg/kg/day), or vehicle (VEH) for 7 days. Baseline activity: Baseline horizontal locomotion (**a**), rearing (**b**) and center duration (**c**) in the open field on treatment day 7 are shown for SAL/VEH (n = 11), AMPH/VEH (n = 12), AMPH/**1a** (n = 12), and AMPH/**16c** (n = 9) groups as a 20 min total activity. AMPH-induced activity: The effects of a challenge AMPH injection (1.5 mg/kg) on horizontal locomotion (**d**), rearing (**e**), and center duration (**f**) are shown in 5 min intervals, and as area under the curve (AUC) total activity (**g**, **h**, **i** respectively). AMPH-induced behaviors are calculated as Δ baseline (vs. last 5 min of baseline). Values are shown as mean ± SEM. * $p < 0.05$, ** $p < 0.01$, *** $p < 0.001$ compared to SAL/VEH. # $p < 0.05$, ## $p < 0.01$, ### $p < 0.001$ compared to AMPH/VEH.

DISCUSSION AND CONCLUSIONS

The combination of 1,4-disubstituted phenylpiperazines with pyrazolo[1,5-*a*]pyridine heterocyles by an appropriate linker led to a series of ligands with subnanomolar affinity for the dopamine D_2R. Intensive pharmacological investigations employing classical [^{35}S]GTPγS binding experiments but also highly sensitive BRET biosensors revealed partial agonist properties for the activation of $G\alpha_{i/o}$ proteins at $D_{2L}R$, $D_{2S}R$ and D_3R. Receptor subtype-selectivity as well as potencies and efficacies could be modulated by the substitution pattern and the attachment of the linker subunit to the pyrazolo[1,5-*a*]pyridine appendage. While substituents in position 2 of the heterocycle or attachment of the linker via an aminocarbonyl moiety led to relatively weak efficacies and/or potencies, oxymethylene spacers and the addition of polar functional groups to position 3 of the heterocycle were highly beneficial for the intrinsic activity of 1,4-DAP-based dopaminergics. Interestingly, the family of phenylpiperazines preferentially activated the $G\alpha_o$ subtypes, with both, higher efficacies and potencies when compared to $G\alpha_i$ activation. At the same time, the compounds bearing either a 2,3-dichloro- or 2-methoxyphenylpiperazine moiety were inhibitors of β-arrestin recruitment at $D_{2L}R$ and $D_{2S}R$, indicating substantial G protein bias.

When the substituted phenylpiperazine unit was replaced by a 5-hydroxy-*N*-propyl-2-aminotetraline group, super-affinity dopamine receptor agonists were discovered. Here, receptor affinities and potencies were only slightly influenced by substitutions at the pyrazolo[1,5-*a*]pyridine appendage, but strongly dependent on the absolute configuration of the stereogenic center. Compounds in the (*S*)-configuration were found to be full agonists for the activation of all signaling pathways at $D_{2S}R$, $D_{2L}R$ and D_3R. In contrast, (*R*)-**13a**,**b** activated G proteins to the full extent, but were only partial agonists for the recruitment of β-arrestins at $D_{2S}R$ and $D_{2L}R$. Although these ligands might not serve as antipsychotics due to their high efficacy for G protein-mediated signaling, they present an interesting starting point for further SAR for understanding the molecular determinants of functional selectivity at the

D_2R, since the same head group in combination with a different lipophilic appendage has previously been reported to disfavor G protein-mediated signaling.[19]

Besides the investigation of receptor activation at the level of G proteins, we examined the effects of **16c**, a representative 2-methoxyphenylpiperazine with high D_2R-affinity, in comparison to the antipsychotic **1a** further downstream at the level of GIRK channels. These K^+-channels have been shown to be highly associated with D_2R[56] and are key inhibitory mediators for the control of electrical excitability.[51] In good agreement with their partial agonist nature observed in biochemical and cell-based assays, **1a** and **16c** were able to mediate submaximal GIRK activation via D_2R stimulation in electrophysiological recordings. Compared to the antipsychotic **1a**, currents elicited by **16c** were stronger and, in good agreement with the higher potencies observed in [^{35}S]GTPγS binding and BRET assays for **16c**, occurred at lower concentrations. However, both phenylpiperazines did not lead to significant activation of GIRK by stimulation of the closely related D_3R subtype. The different behavior in GIRK1/2 activation may reflect the distinct coupling properties of D_2R and D_3R towards the $G\alpha_i$ and $G\alpha_o$ subtypes, and hence lead to a lower degree of overall activation of the G proteins by the partial agonists in D_3R expressing cells.

Motivated by the highly similar *in vitro* profiles of **1a** and **16c**, we investigated whether G protein-biased D_2R partial agonists with pyrazolo[1,5-*a*]pyridine substructure possess antipsychotic activity *in vivo* and could therefore serve as potential novel therapeutics. Thus, we investigated continuously administered **16c** in comparison to **1a** for their influence on schizophrenia-like alterations in rats. Both compounds were able to reverse amphetamine-induced hyper-locomotion, which models the psychotic symptoms of the disease.[74] Furthermore, amphetamine-pretreated animals showed elevated anxiety, which was partially reversed by **16c**, but not **1a**. However, unlike **1a**, **16c** treatment exacerbates the baseline locomotion-related attenuations induced by amphetamine pretreatment. These results indicate that **16c** treatment can effectively improve schizophrenia-like disruptions *in vivo*, but

as a side effect, may reduce general locomotor activity. Nevertheless, given the additional anxiolytic effects, in a personalized medicine approach **16c** may be a specific treatment option for schizophrenia patients with a co-morbid anxiety disorder.[70, 71] However, in our *in vitro* studies, **16c** and **1a** were highly similar, although **16c** displayed a higher preference for $G\alpha_o$ over $G\alpha_i$ activation at D_2R. It will therefore be interesting to further investigate the signaling profiles of **16c** and **1a** *in vitro* and relate them to the differences in the functional responses observed *in vivo*.

Altogether, our study revealed 1,4-DAPs with a pyrazolo[1,5-*a*]pyridine appendage as highly potent G protein-biased partial agonists devoid of β-arrestin recruitment at D_2R. Compounds with this kind of activity profile represent potential novel antipsychotics as we could demonstrate *in vivo* antipsychotic activity for the representative oxime **16c**. Indeed, antagonism of β-arrestin recruitment at D_2R has been identified as common mechanism of clinically effective antipsychotics.[21] Moreover, the pyrazolo[1,5-*a*]pyridine appendage represents a valuable tool for the fine tuning of agonistic and functionally selective properties in conjunction with different orthosteric head groups as illustrated by the different enantiomers of the 5-hydroxy-*N*-propyl-2-aminotetralines.

EXPERIMENTAL SECTION

Chemistry. Reagents and dry solvents were of commercial grade and used as purchased. Reactions requiring anhydrous conditions were carried out under nitrogen atmosphere. MS was run on a Bruker Esquire 2000 by APC or ES ionisatzion. HR-EIMS was run on a JEOL JMS-GC mate II with a solid inlet and EI (70 eV) using Peak-Matching ($M/\Delta M > 5000$) or at the Chair of Organic Chemistry, Friedrich Alexander University Erlangen-Nuremberg on a micrOTOF, source type ESI. NMR spectra were obtained on a Bruker Avance 360 or 600 spectrometer at ambient temperature. ^1H and ^{13}C chemical shifts are reported in ppm (δ) relative to TMS in the solvents indicated. Melting points were

determined with a MEL-TEMP II apparatus (Laboratory Devices, U.S.) in open capillaries. IR spectra were obtained on a Jasco FT/IR 410 or 4100 spectrometer. Purification by column chromatography was performed using silica gel 60. TLC analyses were performed on Merck 60 F254 aluminum sheets and analyzed by UV light (254 nm) or $KMnO_4$ staining. Analytical HPLC was performed on Agilent 1100 or 1200 HPLC systems employing a VWL or DAD detector with a Zorbax eclipse XDB-C8 (4.6 mm × 150mm, 5 µm) column. HPLC purity was measured using the following binary solvent system (system 1): eluent CH_3OH in 0.1 % aqueous formic acid, 10 % 3 min, 10-100 % CH_3OH in 15 min, 100 % for 6 min, flow rate 0.5 mL/min, λ 254 nm. The purity of all test compounds and key intermediates was determined to be > 95 %. Preparative RP-HPLC was performed using an Agilent 1100 preparative series instrument with detection wavelengths set to 220 and 254 nm and a Nucleodur C18 HTec column (32 × 250 mm, 5 µm). Compounds were eluted using the following binary solvent system (method A) at a flow rate of 32 mL/min: Acetonitrile (ACN), water 0.1 % TFA, gradient: 5–50% ACN in 0–20 min, 50–95% ACN in 20–22 min, 95% ACN in 22–25 min, 95–5% ACN in 25–30 min. CHN elementary analyses were performed at the Chair of Organic Chemistry, Friedrich Alexander University Erlangen-Nuremberg.

5-{4-[4-(2,3-Dichlorophenyl)piperazin-1-yl]butyramido}pyrazolo[1,5-*a*]pyridine (6a). A solution of **4a** (252 mg, 0.745 mmol) and HATU (283 mg, 0.745 mmol) in dry DMF (13 mL) was stirred at room temperature for 15 min before DIPEA (0.16 mL, 0.994 mmol) was added. After additional 15 min of stirring, a solution of 5-aminopyrazolo-[1,5-*a*]pyridine (**5**) (66.2 mg, 0.497 mmol) in dry dichloromethane (6.0 mL) was added. After 24 h of stirring at room temperature the mixture was diluted with water (100 mL), adjusted to pH 10 with DIPEA and extracted with dichloromethane. The combined organic layers were dried over $MgSO_4$ and evaporated. The crude product was purified by column chromatography (dichloromethane/methanol 99:1 to 95:5) to yield **6a** as a grey solid (146 mg, 68%). Mp: 117 °C. IR (NaCl): 3389, 2954, 2826, 1646, 1577, 1508, 1447, 1342, 1240, 1190, 1127, 846

cm^{-1}. ^{1}H NMR ($CDCl_3$/CD_3OD, 600 MHz, δ): 2.03 (quin. *J* = 7.3 Hz, 2 H), 2.53 (t, *J* = 7.1 Hz, 2 H), 2.78 (t, *J* = 7.6 Hz, 2 H), 2.95 (m, 4 H), 3.16 (m, 4 H), 6.45 (dd, *J* = 2.3 Hz, 0.8 Hz, 1 H), 6.92 (dd, *J* = 7.6 Hz, 2.5 Hz, 1 H), 7.00 (dd, *J* = 7.4 Hz, 2.1 Hz, 1 H), 7.19 (m, 2 H), 7.87 (d, *J* = 2.5 Hz, 1 H), 8.11 (d, *J* = 1.9 Hz, 1 H), 8.36 (dd, *J* = 7.6 Hz, 0.8 Hz, 1 H), NH n.d. ^{13}C NMR ($CDCl_3$/CD_3OD, 90 MHz, δ): 22.1, 35.1, 50.9, 53.6, 58.2, 97.4, 106.0, 108.0, 119.5, 125.8, 128.1, 128.4, 128.9, 134.7, 135.6, 141.4, 142.9, 151.2, 173.5. HPLC (system 1): t_R = 16.3 min, purity 95%. HR-EIMS: [M^+] calcd for $C_{21}H_{23}N_5OCl_2$, 431.1280; found 431.1280.

5-{4-[4-(2-Methoxyphenyl)piperazin-1-yl]butyramido}pyrazolo[1,5-*a*]pyridine (6b). Compound **6b** was prepared according to the protocol of **6a** using a solution of **4b** (286 mg, 0.952 mmol) and HATU (362 mg, 0.952 mmol) in dry DMF (15 mL) as well as DIPEA (0.20 mL, 1.27 mmol) and 5-aminopyrazolo[1,5-*a*]pyridine (**5**) (84.5 mg, 0.634 mmol) in dichloromethane (6.0 mL). Purification by column chromatography (dichloromethane/methanol 99:1 to 95:5) yielded **6b** as off-white solid (239 mg, 95%). Mp: 95 °C. IR (NaCl) 3773, 3401, 2944, 2833, 1647, 1573, 1526, 1502, 1439, 1343, 1304, 1241, 1118, 1024, 915, 843 cm^{-1}. ^{1}H NMR ($CDCl_3$, 600 MHz, δ) 1.97–2.07 (m, 2 H), 2.65 (t, *J* = 6.3 Hz, 2 H), 2.91 (t, *J* = 5.9 Hz, 2 H), 3.04–3.13 (m, 4 H), 3.21–3.30 (m, 4 H), 3.84 (s, 3 H), 6.37 (dd, *J* = 2.2 Hz, 0.7 Hz, 1 H), 6.78 (dd, *J* = 7.5 Hz, 2.3 Hz, 1 H), 6.85 (dd, *J* = 7.9 Hz, 1.3 Hz, 1 H), 6.88–6.90 (m, 1 H), 6.91 (dd, *J* = 7.8 Hz, 1.3 Hz, 1 H), 7.00–7.05 (m, 1 H), 7.84 (d, *J* = 2.3 Hz, 1 H), 7.90 (d, *J* = 1.9 Hz, 1 H), 8.29 (dt, *J* = 7.4 Hz, 0.7 Hz, 1 H), 8.75 (s, 1 H). ^{13}C NMR ($CDCl_3$, 90 MHz, δ): 20.4, 35.3, 50.8, 53.3, 55.5, 57.7, 96.9, 106.3, 107.0, 111.5, 118.6, 121.2, 124.1, 128.8, 133.4, 139.5, 140.2, 142.7, 152.3, 172.9. HPLC (system 1): t_R = 14.7 min, purity 97%. HR-EIMS: [M^+] calcd for $C_{22}H_{27}N_5O_2$, 393.2165; found 393.2164.

5-{4-[4-(2,3-Dichlorophenyl)piperazin-1-yl]butyramido}pyrazolo[1,5-*a*]pyridine-3-carbaldehyde (7a). A solution of **6a** (183 mg, 0.423 mmol) in dry DMF (2.0 mL) was cooled to 0 °C, before 0.61 mL (1.31 mmol) of a preformed Vilsmeyer reagent (0.4 mL $POCl_3$

in 1.6 mL dry DMF) was added dropwisely. After stirring at room temperature for 1 h, distilled water was added and the mixture was alkalized by addition of 5 M NaOH. The mixture was extracted with chloroform, the combined organic layers were dried over $MgSO_4$ and evaporated. Purification by column chromatography (dichloromethane/methanol 97:3) yielded **7a** as a white solid (114 mg, 59%). Mp: 189 °C. IR (NaCl): 3300, 3248, 3138, 3042, 2936, 2817, 2251, 1695, 1654, 1628, 1527, 1450, 1400, 1195, 959, 879 cm^{-1}. ^1H NMR ($CDCl_3$, 600 MHz, δ) 1.97–2.04 (m, 2 H), 2.57 (t, *J* = 6.8 Hz, 2 H), 2.59 (t, *J* = 6.5 Hz, 2 H), 2.68–2.76 (m, 4 H), 3.10–3.20 (m, 4 H), 7.01 (dd, *J* = 7.6 Hz, 1.8 Hz, 1 H), 7.13 (t, *J* = 7.8 Hz, 1 H), 7.16 (dd, *J* = 8.0 Hz, 1.8 Hz, 1 H) 8.05 (dd, *J* = 7.5 Hz, 1.3 Hz, 1 H), 8.16 (d, *J* = 1.9 Hz, 1 H), 8.32 (s, 1 H), 8.49 (d, *J* = 7.5 Hz, 1 H), 9.93 (br s, 1 H), 9.96 (s, 1 H). ^{13}C NMR ($CDCl_3$, 90 MHz, δ): 21.9, 36.1, 51.3, 53.2, 57.2, 105.6, 109.4, 113.2, 118.8, 124.8, 127.5, 127.5, 129.8, 134.0, 140.4, 141.0, 147.5, 150.9, 172.2, 183.0. HPLC (system 1): t_R = 16.1 min, purity 96%. HR-EIMS: [M^+] calcd for $C_{22}H_{23}N_5O_2Cl_2$, 459.1229; found 459.1228.

5-{4-[4-(2-Methoxyphenyl)piperazin-1-yl]butyramido}pyrazolo[1,5-*a*]pyridine-3-carbaldehyde (7b). Compound **7b** was prepared according to the protocol of compound **7a** using a solution of **6b** (192 mg, 0.488 mmol) in DMF (3.0 mL) and 0.70 mL of the preformed Vilsmeyer reagent (1.51 mmol). Purification by column chromatography (dichloromethane/methanol 97:3) yielded **7b** as light yellow solid (118 mg, 58%). Mp: 108 °C. IR (NaCl) 3403, 2021, 2950, 2820, 1660, 1635, 1579, 1529, 1500, 1482, 1460, 1403, 1368, 1300, 1240, 1196, 1022, 916, 847 cm^{-1}. ^1H NMR ($CDCl_3$, 600 MHz, δ): 1.98–2.04 (m, 2 H), 2.60 (t, *J* = 6.9 Hz, 2 H), 2.64 (t, *J* = 7.1 Hz, 2 H), 2.72–2.80 (m, 4 H), 3.14–3.20 (m, 4 H), 3.86 (s, 3 H), 6.86 (dd, *J* = 8.1 Hz, 1.4 Hz, 1 H), 6.91 (ddd, *J* = 7.6 Hz, 7.6 Hz, 1.4 Hz, 1 H), 6.96 (dd, *J* = 7.9 Hz, 1.7 Hz, 1 H), 7.00 (ddd, *J* = 7.8 Hz, 7.5 Hz, 1.6 Hz, 1 H), 7.94 (dd, *J* = 7.6 Hz, 1.9 Hz, 1 H), 8.29 (s, 1 H), 8.34 (d, *J* = 2.1 Hz, 1 H), 8.45 (d, *J* = 7.6 Hz, 1 H), 9.93 (s, 1 H), 10.48 (br s, 1 H). ^{13}C NMR ($CDCl_3$, 90 MHz, δ): 21.9, 25.6, 50.4, 53.3, 55.4, 57.2, 105.4, 109.6, 111.3, 113.2, 118.3, 121.0, 123.1, 129.6, 140.5, 141.0, 141.2, 147.3, 152.2,

172.7, 182.8. HPLC (system 1): t_R = 14.5 min, purity 97%. HR-EIMS: [M^+] calcd for $C_{23}H_{27}N_5O_3$, 421.2114; found 421.2117.

5-{4-[4-(2,3-Dichlorophenyl)piperazin-1-yl]butyramido}pyrazolo[1,5-*a*]pyridine-3-carbaldehydoxime (8a). A solution of hydroxylamine hydrochloride (34.6 mg, 0.498 mmol) in distilled water (1.4 mL) and 2 M NaOH (0.25 mL, 0.50 mmol) was cooled to 0 °C and adjusted to pH 5.0 by addition of 2 M HCl, before a solution of **7a** (115 mg, 0.249 mmol) in ethanol (12.4 mL) was added and the mixture was heated to reflux for 2 h. After cooling, saturated $NaHCO_3$ solution was added and the mixture was extracted with CH_2Cl_2. The combined organic layers were dried ($MgSO_4$) and concentrated in vacuo. Purification by column chromatography (dichloromethane/methanol 97:3 to 95:5) yielded **8a** as white solid (91.7 mg, 77% as mixture of two isomers in a 50% to 50% ratio). Mp: 146 °C. IR (NaCl) 3214, 2823, 2359, 1646, 1576, 1506, 1449, 1353, 1241, 1211, 1130, 961 cm^{-1}. ^1H NMR (DMSO-d_6, 600 MHz, δ): (Isomer 1, 50%) 1.76–1.85 (m, 2 H), 2.37–2.46 (m, 4 H), 2.51–2.56 (m, 4 H), 2.91–2.97 (m, 4 H), 7.02 (dd, *J* = 7.9 Hz, 2.1 Hz, 1 H), 7.08 (dd, *J* = 7.4 Hz, 2.3 Hz, 1 H), 7.21–7.28 (m, 2 H), 7.54 (s, 1 H), 8.36 (d, *J* = 2.5 Hz, 1 H), 8.58 (d, *J* = 2.5 Hz, 1 H), 8.64 (d, *J* = 7.6 Hz, 1 H), 10.35 (s, 1 H), 11.21 (s, 1 H); (Isomer 2 50%) 1.76–1.85 (m, 2 H), 2.37–2.46 (m, 4 H), 2.51-2.56 (m, 4 H), 2.91–2.97 (m, 4 H), 7.02 (dd, *J* = 7.9 Hz, 2.1 Hz, 1 H), 7.03 (dd, *J* = 7.5 Hz, 2.4 Hz, 1 H), 7.21–7.28 (m, 2 H), 8.08 (s, 1 H), 8.22 (s, 1 H), 8.55 (d, *J* = 2.5 Hz, 1 H), 8.65 (d, *J* = 7.6 Hz, 1 H), 10.32 (s, 1 H), 10.71 (s, 1 H). ^{13}C NMR (DMSO-d_6, 90 MHz, δ): (Isomer 1, 50%) 22.0, 34.5, 50.9, 52.7, 57.1, 101.9, 102.7, 107.8, 119.4, 124.3, 126.0, 128.3, 129.5, 132.5, 136.0, 137.1, 138.7, 145.0, 151.2, 172.1; (Isomer 2 50%) 22.0, 34.5, 50.9, 52.7, 57.1, 104.2, 104.5, 107.7, 119.4, 124.3, 126.0, 128.3, 129.5, 132.5, 136.9, 137.1, 142.1, 143.1, 151.2, 171.9. HPLC (system 1): t_R = 15.8 min, purity 96%. HR-EIMS: [M^+] calcd for $C_{22}H_{24}N_6O_2Cl_2$, 474.1338; found 474.1338.

5-{4-[4-(2-Methoxyphenyl)piperazin-1-yl]butyramido}pyrazolo[1,5-*a*]pyridine-3-carbaldehydoxime (8b). Compound **8b** was prepared according to the protocol of **8a** using a

solution of hydroxylamine hydrochloride (36.9 mg, 0.53 mmol) in distilled water (1.5 mL) and 2 M NaOH (0.27 mL, 0.53 mmol) as well as a solution of **7b** (112 mg, 0.265 mmol) in ethanol (13.1 mL). Purification by column chromatography (dichloromethane/methanol 98:2 to 95:5) yielded **8b** as light yellow solid (108 mg, 83% mixture of two isomers in a 50% to 50% ratio). Mp: 118 °C. IR (NaCl): 3398, 3021, 1646, 1581, 1502, 1463, 1355, 1243, 1180, 1117, 1021, 915, 866 cm^{-1}. ^1H NMR ($CDCl_3$, 600 MHz, δ): (Isomer 1, 50%) 1.99–2.09 (m, 2 H), 2.54–2.63 (m, 4 H), 2.73–2.81 (m, 4 H), 3.15–3.25 (m, 4 H), 3.87 (s, 3 H), 6.88 (dd, *J* = 7.9 Hz, 1.2 Hz, 1 H), 6.88–6.96 (m, 2 H), 6.97–7.02 (m, 1 H), 7.22 (dd, *J* = 7.6 Hz, 2.4 Hz, 1 H), 7.57 (s, 1 H), 8.11 (dd, *J* = 2.4 Hz, 0.7 Hz, 1 H), 8.30 (dd, *J* = 7.5 Hz, 0.7 Hz, 1 H), 8.73 (s, 1 H), 9.51 (br s, 1 H), free OH n. d.; (Isomer 2, 50%) 1.99–2.09 (m, 2 H), 2.54–2.63 (m, 4 H), 2.73–2.81 (m, 4 H), 3.15–3.25 (m, 4 H), 3.87 (s, 3 H), 6.86 (dd, *J* = 7.9 Hz, 1.2 Hz, 1 H), 6.88–6.96 (m, 2 H), 6.97–7.02 (m, 1 H), 7.03 (dd, *J* = 7.6 Hz, 2.3 Hz, 1 H), 7.95 (s, 1 H), 8.13 (dd, *J* = 2.4 Hz, 0.7 Hz, 1 H), 8.26 (s, 1 H), 8.35 (dd, *J* = 7.5 Hz, 0.7 Hz, 1 H), 9.38 (b s, 1 H), free OH n. d. ^{13}C NMR ($CDCl_3$, 90 MHz, δ): (Isomer 1, 50%) 22.0, 35.9, 50.1, 53.4, 55.4, 57.5, 104.3, 104.5, 107.9, 111.3, 118.2, 121.0, 123.1, 129.0, 137.5, 137.9, 141.0, 143.4, 143.4, 152.2, 172.5; (Isomer 2, 50%) 22.0, 35.6, 49.9, 53.3, 55.4, 57.5, 103.0, 103.4, 108.3, 111.3, 118.2, 121.0, 123.1, 129.1, 137.6, 139.7, 141.0, 146.1, 136.9, 152.2, 172.7. HPLC (system 1): t_R = 12.5 min, purity 100%. HR-EIMS: [M^+] calcd for $C_{23}H_{28}N_6O_3$, 436.2223; found 436.2222.

5-{4-[4-(2,3-Dichlorophenyl)piperazin-1-yl]butyramido}pyrazolo[1,5-*a*]pyridine-3-carbonitrile (9a). A solution of TCT (46.4 mg, 0.25 mmol) in DMF (1.0 mL) was stirred at room temperature for 1 h. Subsequently, 0.54 mL of the preformed TCT/DMF complex were added to a solution of **8a** (60.1 mg, 127 µmol) in DMF (1.6 mL). After stirring at room temperature for 5 h, the mixture was diluted with saturated sodium bicarbonate solution and extracted with $CHCl_3$. The combined organic layers were dried ($MgSO_4$) and evaporated. The residue was purified by chromatography (dichloromethane/methanol 98:2 to 95:5) to yield **9a**

as light yellow solid (43.6 mg, 75%). Mp: 180 °C. IR (NaCl): 3305, 3069, 2942, 2819, 2218, 1697, 1650, 1577, 1532, 1510, 1450, 1421, 1240, 1045, 960 cm^{-1}. ^1H NMR ($CDCl_3$, 600 MHz, δ): 2.03–2.09 (m, 2 H), 2.59 (t, *J* = 6.8 Hz, 2 H), 2.69 (t, *J* = 6.4 Hz, 2 H), 2.80–2.90 (m, 4 H), 3.13–3.23 (m, 4 H), 6.98 (dd, *J* = 7.7 Hz, 1.8 Hz, 1 H), 7.17 (t, *J* = 7.8 Hz, 1 H), 7.20 (dd, *J* = 8.0 Hz, 1.8 Hz, 1 H), 7.35 (dd, *J* = 7.5 Hz, 2.2 Hz, 1 H), 8.04 (d, *J* = 2.1 Hz, 1 H), 8.16 (s, 1 H), 8.44 (d, *J* = 7.6 Hz, 1 H), 9.40 (s, 1 H). ^{13}C NMR ($CDCl_3$, 90 MHz, δ): 21.6, 35.7, 50.6, 53.0, 57.0, 81.5, 103.4, 108.9, 114.1, 118.7, 125.2, 127.6, 127.6, 130.0, 134.2, 138.7, 143.3, 145.9, 150.5, 171.8. HPLC (system 1): t_R = 16.8 min, purity 97%. HR-EIMS: [M^+] calcd for $C_{22}H_{22}N_6OCl_2$, 456.1232; found 456.1232.

5-{4-[4-(2-Methoxyphenyl)piperazin-1-yl]butyramido}pyrazolo[1,5-*a*]pyridine-3-carbonitrile (9b). A solution of **8b** (22.0 mg, 50 μmol) in acetic acid anhydride (2.0 mL) was heated to reflux for 6 h. After cooling, the mixture was diluted with ice water and extracted with $CHCl_3$. The combined organic layers were dried ($MgSO_4$) and evaporated under vacuo. Purification by column chromatography (dichloromethane/methanol 98:2 to 95:5) yielded **9b** as colorless oil (2.5 mg, 12%). IR (NaCl): 2960, 2819, 2218, 1698, 1649, 1582, 1534, 1501, 1454, 1241, 1025 cm^{-1}. ^1H NMR ($CDCl_3$, 600 MHz, δ): 2.03–2.09 (m, 2 H), 2.62 (t, *J* = 6.8 Hz, 2 H), 2.74 (t, *J* = 6.4 Hz, 2 H), 2.87–2.92 (m, 4 H), 3.18–3.29 (m, 4 H), 3.87 (s, 3 H), 6.88 (dd, *J* = 8.2 Hz, 1.2 Hz, 1 H), 6.93–6.96 (m, 2 H), 7.02–7.06 (m, 1 H), 7.26 (dd, *J* = 7.6 Hz, 2.3 Hz, 1 H), 8.15 (s, 1 H), 8.17 (dd, *J* = 2.3 Hz, 0.8 Hz, 1 H), 8.41 (dd, *J* = 7.6 Hz, 0.8 Hz, 1 H), 9.71 (bs, 1 H). ^{13}C NMR ($CDCl_3$, 90 MHz, δ): 21.4, 35.5, 49.5, 53.0, 55.4, 56.7, 81.6, 103.6, 108.9, 111.4, 114.1, 118.4, 121.2, 123.7, 129.9, 138.6, 140.2, 143.3, 145.9, 152.2, 171.8. HPLC (system 1): t_R = 15.0 min, purity 99%. HR-EIMS: [M^+] calcd for $C_{23}H_{26}N_6O_2$, 418.2117; found 418.2116.

6-{4-[4-(2-Methoxyphenyl)piperazin-1-yl]butoxy}lpyrazolo[1,5-*a*]pyridine (12a). A solution of **10a** (40 mg, 0.149 mmol) and NaI (33.5 mg, 0.223 mmol) in acetonitrile (0.9 mL) was heated to 85 °C for 30 min, before 1-(2-methoxyphenyl)piperazine (31.4 mg, 0.164

mmol) and triethylamine (0.05 mL, 0.316 mmol) were added and the mixture was stirred at 85 °C for another 5 h. After cooling, saturated $NaHCO_3$ solution was added and the mixture was extracted with CH_2Cl_2. The combined organic layers were dried (Na_2SO_4) and evaporated in vacuo. Purification of the residue by column chromatography (dichloromethane/methanol 98:2 to 95:5) yielded **12a** as off-white oil (50.0 mg, 89%). IR (NaCl): 3108, 2942, 2817, 1643, 1499, 1292, 1240, 1199, 748 cm^{-1}. ^1H NMR ($CDCl_3$, 600 MHz, δ): 1.80–1.85 (m, 2 H), 1.87–1.91 (m, 2 H), 2.59 (t, *J* = 7.6 Hz, 2 H), 2.77–2.82 (m, 4 H), 3.17–3.22 (m, 4 H), 3.86 (s, 3 H), 3.99 (t, *J* = 6.3 Hz, 2 H), 6.45 (d, *J* = 2.1 Hz, 1 H), 6.87 (dd, *J* = 7.9 Hz, 1.0 Hz, 1 H), 6.91–6.93 (m, 2 H), 6.95 (dd, *J* = 7.5 Hz, 2.0 Hz, 1 H), 7.01 (ddd, *J* = 7.9 Hz, 7.0 Hz, 2.0 Hz, 1 H), 7.41 (d, *J* = 9.6 Hz, 1 H), 7.84 (d, *J* = 2.2 Hz, 1 H), 8.06–8.07 (m, 1 H). ^{13}C NMR ($CDCl_3$, 90 MHz, δ): 23.1, 27.1, 50.2, 53.4, 55.4, 58.1, 68.7, 96.7, 111.2, 111.8, 117.9, 118.4, 119.1, 121.1, 123.2, 136.5, 140.8, 141.0, 148.3, 152.3. HPLC (system 1): t_R = 17.5 min, purity 100%. HR-EIMS: [M^+] calcd for $C_{22}H_{28}N_4O_2$, 380.2212; found 380.2214.

5-{4-[4-(2-Methoxyphenyl)piperazin-1-yl]butoxy}lpyrazolo[1,5-*a*]pyridine (12b). Compound **12b** was synthesized according to the protocol of **12a** employing a solution of **10b** 200 mg, 0.74 mmol) and sodium iodide (167 mg, 1.1 mmol) in acetonitrile (3.3 mL) as well as 1-(2-methoxyphenyl)piperazine (157 mg, 0.818 mmol) and triethylamine (0.11 mL, 0.818 mmol). Purification by column chromatography (hexanes/ethylacetate 1:9) afforded **12b** as off-white solid (252 mg, 89%). Mp: 121 °C, IR (NaCl) 3098, 2942, 2815, 16448, 1500, 1291, 1241, 1228, 1190, 748 cm^{-1}. ^1H NMR ($CDCl_3$, 600 MHz, δ): 1.71–1.76 (m, 2 H), 1.85–1.90 (m, 2 H), 2.49 (t, *J* = 7.6 Hz, 2 H), 2.66–2.70 (m, 4 H), 3.08–3.14 (m, 4 H), 3.86 (s, 3 H), 4.02 (t, *J* = 6.3 Hz, 2 H), 6.29–6.30 (m, 1 H), 6.44 (dd, *J* = 7.6 Hz, 2.6 Hz, 1 H), 6.73 (d, *J* = 2.6 Hz, 1 H), 6.86 (dd, *J* = 7.8 Hz, 0.9 Hz, 1 H), 6.92 (ddd, *J* = 7.5 Hz, 7.0 Hz, 0.9 Hz, 1 H), 6.95 (dd, *J* = 7.5 Hz, 1.7 Hz, 1 H) 7.00 (ddd *J* = 7.8 Hz, 7.0 Hz, 1.7 Hz, 1 H), 7.84 (d, *J* = 2.1 Hz, 1 H), 8.28 (d, *J* = 7.6 Hz, 1 H). ^{13}C NMR ($CDCl_3$, 90 MHz, δ): 23.5, 27.0, 50.7, 53.5, 55.4, 58.2, 68.0, 95.3, 95.4, 106.7, 111.2, 118.2, 121.0, 122.9, 129.3, 141.1, 141.3, 142.7,

152.3, 155.7. ESI-MS: *m/z* 380.0 [M^+]. Anal. calcd (%) for $C_{22}H_{28}N_4O_2$ x 0.3 H_2O: C 68.48, H 7.47, N 14.52; found: C 68.51, H 7.71, N 14.38.

Ethyl 5-{4-[4-(2-methoxyphenyl)piperazin-1-yl]butoxy}lpyrazolo[1,5-*a*]pyridine-2-carboxylate (12c). Compound **12c** was synthesized according to the protocol of **12a** using a solution of **10c** (302 mg, 0.885 mmol) and sodium iodide (199 mg, 1.33 mmol) in acetonitrile (5.0 mL) as well as a solution of 1-(2-methoxyphenyl)piperazine (187 mg, 0.973 mmol) and triethylamine (0.14 mL, 1.01 mmol) in acetonitrile (2.0 mL) and allowing a reaction time of 8 h. Purification by column chromatography (dichloromethane/methanol 98:2) yielded **12c** as light yellow solid (350 mg, 87%). Mp: 105 °C. IR (NaCl): 2941, 2813, 1720, 1649, 1593, 1539, 1499, 1448, 1406, 1302, 1240, 1147, 1099, 1026, 981, 925, 819 cm^{-1}. ^1H NMR ($CDCl_3$, 600 MHz, δ): 1.44 (t, *J* = 7.1 Hz, 3 H), 1.68–1.79 (m, 2 H), 1.83–1.94 (m, 2 H), 2.50 (t, *J* = 7.4 Hz, 2 H), 2.63–2.73 (m, 4 H), 3.06–3.18 (m, 4 H), 3.87 (s, 3 H), 4.03 (6, *J* = 6.3 Hz, 2 H), 4.46 (q, *J* = 7.1 Hz, 2 H), 6.58 (dd, *J* = 7.7 Hz, 2.7 Hz, 1 H), 6.76 (d, *J* = 2.5 Hz, 1 H), 6.86 (d, *J* = 0.8 Hz, 1 H), 6.86 (dd, *J* = 7.8 Hz, 1.3 Hz, 1 H), 6.91 (ddd, *J* = 7.9 Hz, 6.6 Hz, 1.3 Hz, 1 H), 6.95 (dd, *J* = 7.9 Hz, 2.7 Hz, 1 H), 7.00 (ddd, *J* = 7.8 Hz, 6.5 Hz, 2.6 Hz, 1 H), 8.34 (dt, *J* = 7.7 Hz, 0.7 Hz, 1 H). ^{13}C NMR ($CDCl_3$, 150 MHz, δ): 14.4, 23.4, 26.9, 50.7, 53.5, 55.3, 58.2, 61.3, 68.3, 95.9, 98.6, 109.5, 111.2, 118.2, 121.0, 122.9, 129.6, 141.3, 141.9, 145.8, 152.3, 156.0, 162.9. HPLC (system 1): t_R = 15.7 min, purity 99%. HR-EIMS: [M^+] calcd for $C_{25}H_{32}N_4O_4$, 452.2424; found 452.2423.

5-{4-[4-(2-Methoxyphenyl)piperazin-1-yl]butoxy}-2-hydroxymethylpyrazolo[1,5-*a*]pyridine (12d). To a solution of **12c** (230 mg, 0.508 mmol) in diethyl ether (25 mL) was added a solution of $LiAlH_4$ in diethyl ether (4 M, 130 µL, 0.508 mmol). After stirring at 0 °C for 1 h and at room temperature for 2 h, the reaction was quenched by addition of saturated $NaHCO_3$ solution. After extraction with CH_2Cl_2, the combined organic layers were dried ($MgSO_4$) and evaporated. Purification by column chromatography (dichloromethane/methanol 95:5) yielded **12d** as light yellow solid (155 mg, 74%). Mp: 48

°C. IR (NaCl): 3328, 2937, 2818, 1648, 1593, 1541, 1500, 1445, 1300, 1240, 1202, 1116, 1028, 817 cm^{-1}. ^1H NMR ($CDCl_3$, 600 MHz, δ): 1.71–1.77 (m, 2 H), 1.84–1.90 (m, 2 H), 2.51 (t, *J* = 7.6 Hz, 2 H), 2.65–2.73 (m, 4 H), 3.07–3.17 (m, 4 H), 3.86 (s, 3 H), 4.01 (t, *J* = 6.3 Hz, 2 H), 4.84 (s, 2 H), 6.28 (s, 1 H), 6.42 (dd, *J* = 7.6 Hz, 2.6 Hz, 1 H), 6.68 (d, *J* = 2.6 Hz, 1 H), 6.86 (dd, *J* = 8.1 Hz, 1.3 Hz, 1 H), 6.92 (ddd, *J* = 7.8 Hz, 6.9 Hz, 1.3 Hz, 1 H), 6.95 (dd, *J* = 7.9 Hz, 2.1 Hz, 1 H), 7.00 (ddd, *J* = 8.0 Hz, 7.1 Hz, 2.0 Hz, 1 H), 8.20 (d, *J* = 7.6 Hz, 1 H), free OH n. d. ^{13}C NMR ($CDCl_3$, 90 MHz, δ): 23.3, 27.0, 50.6, 53.5, 55.4, 58.2, 59.5, 68.0, 93.5, 95.3, 106.7, 111.2, 118.2, 121.0, 123.0, 129.2, 141.3, 142.2, 152.3, 155.7, 155.9. HPLC (system 1): t_R = 13.9 min, purity 96%. HR-EIMS: [M^+] calcd for $C_{23}H_{30}N_4O_3$, 410.2318; found 410.2318.

5-{4-[4-(2-Methoxyphenyl)piperazin-1-yl]butoxy}pyrazolo[1,5-*a*]pyridine-2-carbaldehyde (12e). A suspension of **12d** (125 mg, 0.305 mmol) and MnO_2 (266 mg, 3.05 mmol) in dichloromethane (12 mL) was stirred at room temperature for 14 h. After filtration, the filtrate was evaporated and the residue was purified by column chromatography (dichloromethane/methanol/dimethyl ethylamine 99:0.5:0.5) to give **12e** as yellow solid (121 mg, 97%). Mp: 98 °C. IR (NaCl): 2940, 2874, 2812, 1699, 1648, 1593, 1540, 1499, 1446, 1240, 1207, 1147, 1026 cm^{-1}. ^1H NMR ($CDCl_3$, 600 MHz, δ): 1.70–1.80 (m, 2 H), 1.85–1.95 (m, 2 H), 2.50 (t, *J* = 7.5 Hz, 2 H), 2.63–2.73 (m, 4 H), 3.06–3.17 (m, 4 H), 3.86 (s, 3 H), 4.04 (t, *J* = 6.4 Hz, 2 H), 6.42 (dd, *J* = 7.6 Hz, 2.6 Hz, 1 H), 6.79 (d, *J* = 2.4 Hz, 1 H), 6.81 (d, *J* = 0.8 Hz, 1 H), 6.86 (dd, *J* = 7.8 Hz, 1.2 Hz, 1 H), 6.92 (ddd, *J* = 7.8 Hz, 6.5 Hz, 1.3 Hz, 1 H), 6.95 (dd, *J* = 7.9 Hz, 2.5 Hz, 1 H), 7.00 (ddd, *J* = 7.9 Hz, 6.5 Hz, 2.5 Hz, 1 H), 8.30 (dt, *J* = 7.6 Hz, 0.8 Hz, 1 H), 10.13 (s, 1 H). ^{13}C NMR ($CDCl_3$, 90 MHz, δ): 23.4, 26.9, 50.6, 53.5, 55.4, 58.2, 68.3, 95.5, 96.3, 110.3, 111.2, 118.2, 121.0, 122.9, 129.6, 141.3, 142.3, 152.3, 152.4, 156.2, 187.8. HPLC (system 1): t_R = 14.5 min, purity 95%. HR-EIMS: [M^+] calcd for $C_{23}H_{28}N_4O_3$, 408.2161; found 408.2162.

5-{4-[4-(2-Methoxyphenyl)piperazin-1-yl]butoxy}pyrazolo[1,5-*a*]pyridine-2-aldehydoxime (12f). A solution of hydroxylamine hydrochloride (53.3 mg, 0.752 mmol) in distilled water (2.1 mL) and 2 M NaOH (0.38 mL, 0.76 mmol) was cooled to 0 °C and adjusted to pH 5.0 by addition of 2 M HCl. Subsequently a solution of **12e** (154 mg, 0.376 mmol) in ethanol (16.5 mL) was added and the mixture was heated to reflux for 2 h. After cooling and addition of saturated $NaHCO_3$ solution, the mixture was extracted with CH_2Cl_2. The combined organic layers were dried ($MgSO_4$) and evaporated. Purification by column chromatography (dichloromethane/methanol 98:2 to 95:5) yielded **12f** as white solid (136 mg, 85% mixture of two isomers in an 80% to 20% ratio). Mp: 138 °C. IR (NaCl): 3189, 2941, 2874, 2828, 1647, 1593, 1540, 1499, 1450, 1388, 1241, 1207, 1117, 1025, 974, 911, 811 cm^{-1}. ^1H NMR ($CDCl_3$, 600 MHz, δ): (major isomer) 1.76–1.83 (m, 2 H), 1.85–1.92 (m, 2 H), 2.54 (t, *J* = 7.5 Hz, 2 H), 2.71–2.80 (m, 4 H), 3.09–.20 (m, 4 H), 3.87 (s, 3 H), 4.00 (t, *J* = 6.2 Hz, 2 H), 6.44 (dd, *J* = 7.6 Hz, 2.6 Hz, 1 H), 6.50 (s, 1 H), 6.63 (d, *J* = 2.3 Hz, 1 H), 6.86 (dd, *J* = 8.0 Hz, 1.2 Hz, 1 H), 6.92 (ddd, *J* = 7.7 Hz, 7.3 Hz, 1.4 Hz, 1 H), 6.96 (dd, *J* = 7.9 Hz, 1.9 Hz, 1 H), 7.00 (ddd, *J* = 7.9 Hz, 7.3 Hz, 1.7 Hz, 1 H), 8.19 (d, *J* = 7.6 Hz, 1 H), 8.25 (s, 1 H), free OH n. d.; (minor isomer) 1.76–1.83 (m, 2 H), 1.85–1.92 (m, 2 H), 2.54 (t, *J* = 7.5 Hz, 2 H), 2.71–2.80 (m, 4 H), 3.09–3.20 (m, 4 H), 3.87 (s, 3 H), 4.00 (t, *J* = 6.2 Hz, 2 H), 6.55 (dd, *J* = 7.6 Hz, 2.6 Hz, 1 H), 6.74 (d, *J* = 2.5 Hz, 1 H), 6.82 (s, 1 H), 6.86 (dd, *J* = 8.0 Hz, 1.2 Hz, 1 H), 6.92 (ddd, *J* = 7.7 Hz, 7.3 Hz, 1.4 Hz, 1 H), 6.96 (dd, *J* = 7.9 Hz, 1.9 Hz, 1 H), 7.00 (ddd, *J* = 7.9 Hz, 7.3 Hz, 1.7 Hz, 1 H), 7.70 (s, 1 H), 8.23 (d, *J* = 7.6 Hz, 1 H), free OH n. d. ^{13}C NMR ($CDCl_3$, 90 MHz, δ): (major isomer) 23.2, 26.9, 50.4, 53.5, 55.4, 58.1, 68.0, 93.2, 95.2, 107.6, 111.2, 118.3, 121.0, 123.0, 129.0, 141.2, 141.3, 142.0, 146.4, 152.3, 156.1; (minor isomer) 23.2, 26.9, 50.5, 53.5, 55.4, 58.1, 68.2, 95.6, 98.6, 108.9, 111.2, 118.3, 121.0, 123.0, 129.2, 141.2, 141.3, 142.0, 148.5, 152.3, 156.1. HPLC (system 1): t_R = 14.8 min, purity 95%. HR-EIMS: [M^+] calcd for $C_{23}H_{29}N_5O_3$, 423.2270; found 423.2271.

5-{4-[4-(2-Methoxyphenyl)piperazin-1-yl]butoxy}pyrazolo[1,5-*a*]pyridin-2-carbonitrile (12g). A solution of TCT (46.4 mg, 0.25 mmol) in DMF (1.0 mL) was stirred at room temperature. Subsequently, 0.27 mL of this preformed complex were added to a solution of **12f** (29.1 mg, 69 μmol) in DMF (0.8 mL). After stirring at room temperature for 7 h, the reaction was quenched by addition of saturated $NaHCO_3$ solution and extracted with CHCl3. The combined organic layers were dried ($MgSO_4$) and evaporated. Purification by column chromatography (dichloromethane/methanol 99:1) yielded **12g** as white solid (15.1 mg, 54%). IR (NaCl): 2922, 2855, 2806, 2359, 1648, 1593, 1499, 1428, 1379, 1240, 1208, 1115 cm-1. ^{1}H NMR (CD_3OD, 600 MHz, δ): 1.82–1.89 (m, 2 H), 1.89–1.94 (m, 2 H), 2.80 (t, *J* = 7.6 Hz, 2 H), 2.93–3.02 (m, 4 H), 3.11–3.20 (m, 4H), 3.85 (s, 3H), 4.13 (t, *J* = 6.0 Hz, 2 H), 6.80 (dd, *J* = 7.6 Hz, 2.7 Hz, 1 H), 6.88 (d, *J* = 0.8 Hz, 1 H), 6.91 (ddd, *J* = 7.8 Hz, 7.4 Hz, 1.9 Hz, 1 H), 6.96 (dd, *J* = 8.2 Hz, 1.4 Hz, 1 H), 6.97 (dd, *J* = 7.8 Hz, 1.6 Hz, 1 H), 7.03 (ddd, *J* = 8.1 Hz, 7.4 Hz, 1.7 Hz, 1 H), 8.45 (dt, *J* = 7.6 Hz, 0.8 Hz, 1 H). ^{13}C NMR (CD_3OD, 150 MHz, δ): 23.3, 27.6, 50.6, 54.0, 56.0, 58.7, 69.4, 97.2, 102.5, 111.7, 112.9, 115.2, 119.6, 122.2, 125.1, 128.0, 130.7, 141.6, 143.4, 154.0, 158.3. HPLC (system 1) t_R = 15.1 min, purity 100%. HR-EIMS: [M^+] calcd for $C_{23}H_{27}N_5O_2$, 405.2165; found 405.2165.

(*S*)-6-{Propyl[4-(pyrazolo[1,5-*a*]pyridin-6-yloxy)butyl]amino}-5,6,7,8-tetrahydro naphthalen-1-ol (*(S)*-13a). Compound **11a** (9.2 mg, 0.034 mmol) was dissolved in 3 mL acetonitrile and KI (8.5 mg, 0.051 mmol) was added and the mixture was refluxed for 30 mins. Then DIPEA (8.4 μL, 0.051 mmol) and a solution of *(S)*-**10b** (9.0 mg, 0.044 mmol) in 1 mL acetonitrile were added and the reaction mixture was heated at 85 °C for 16 h. The reaction was quenched with water and extracted three times with ethyl acetate. The organic layer was dried over anhydrous Na_2SO_4 and evaporated in vacuo. Preparative HPLC purification employing method A (t_R = 19.5 min), yielded 8 mg (60%) of *(S)*-**13a** as colourless oil. ^{1}H NMR (600 MHz, CD_3OD, δ): 1.06 (t, *J* = 7.3 Hz, 3 H), 1.77–1.87 (m, 2 H), 1.91–2.05 (m, 6 H), 2.35 (bs, 1 H), 2.63–2.69 (m, 2 H), 3.07–3.22 (m, 4 H), 3.41–3.48 (m, 1

H), 3.73–3.77 (m, 1 H), 4.14 (bs, 2 H), 6.61–6.64 (m, 2 H), 6.95–6.98 (m, 2 H), 7.04 (d, J = 9.4 Hz, 1 H), 7.79 (s, 1 H), 8.17 (s, 1 H), 8.43 (s, 1 H). ^{13}C NMR (90 MHz, CD_3OD, δ): 11.3, 19.9, 23.2, 23.7, 25.0, 27.3, 30.9, 52.0, 54.1, 61.9, 69.2, 112.7, 113.6, 119.7, 120.4, 121.2, 123.1, 128.1, 134.7, 147.6, 149.9, 156.2, 159.7. HPLC (system 1) t_R = 17.8 min, purity 99%. $[\alpha]_{589}$ = -36.0° (21 °C, c 0.5, MeOH). HRMS-ESI: [M+H$^+$] calcd for $C_{24}H_{32}N_3O_2$, 394.2489; found 394.2488. *(R)*-**13a** (8 mg, 19%, $[\alpha]_{589}$ = +34.1° (21 °C, c 0.16, MeOH) was prepared from *(R)*-**10b** (17.2 mg, 0.08 mmol) as described above for *(S)*-**13a**.

(*S*)-6-{Propyl[4-(pyrazolo[1,5-*a*]pyridin-5-yloxy)butyl]amino}-5,6,7,8-tetrahydro naphthalen-1-ol (*(S)*-13b). Compound **11b** (48 mg, 0.18 mmol) was dissolved in 5 mL acetonitrile and KI (44.4 mg, 0.27 mmol) was added and the mixture was refluxed for 30 min. Then DIPEA (32 µL, 0.19 mmol) and a solution of *(S)*-**10b** (54.9 mg, 0.27 mmol) in 1 mL acetonitrile were added and the reaction mixture was heated at 85 °C for 16 h. The reaction was quenched with water and extracted three times with ethyl acetate. The organic layer was dried over anhydrous Na_2SO_4 and evaporated in vacuo. Column chromatographic purification using ethyl acetate and 0.1% ammonia yielded *(S)*-**13b** as colorless oil (16 mg, 23%). ^{1}H NMR (600 MHz, CD_3OD, δ): 0.92 (t, J = 7.2 Hz, 3 H), 1.50–1.60 (m, 3 H), 1.67–1.72 (m, 2 H), 1.83–1.88 (m, 2 H), 2.07–2.12 (m, 1 H), 2.47–2.52 (m, 1 H), 2.55–2.57 (m, 2 H), 2.66–2.69 (m, 2 H), 2.71–2.75 (m, 1 H), 2.81–2.85 (m, 1 H), 2.92–2.99 (m, 2 H), 4.06 (t, J = 6.2 Hz, 2 H), 6.37 (dd, J = 0.8, 2.3 Hz, 1 H), 6.53–6.55 (m, 3 H), 6.88 (t, J = 7.7 Hz, 1 H), 6.94 (d, J = 2.5 Hz, 1 H), 7.82 (d, J = 2.3 Hz, 1 H), 8.3 (d, J = 7.7 Hz, 1 H). ^{13}C NMR (150 MHz, CD_3OD, δ): 12.3, 22.5, 24.8, 25.8, 26.7, 28.0, 33.1, 51.3, 53.7, 58.2, 69.4, 96.7, 108.5, 112.7, 121.6, 124.3, 127.2, 129.9, 138.6, 142.9, 143.3, 155.9, 157.5. HPLC (system 1) t_R = 14.7 min, purity 96%. $[\alpha]_{589}$ = -36.0° (26 °C, c 0.64, MeOH). ESI-MS: *m/z* 394.8 [M+H$^+$]. HRMS-ESI: [M+H$^+$] calcd for $C_{24}H_{32}N_3O_2$, 394.2489; found 394.2488. *(R)*-**13b** (8 mg, 19%, $[\alpha]_{589}$ = +26.5° (20 °C, c 0.67, MeOH) was prepared from *(R)*-**10b** (22.9 mg, 0.11 mmol) as described above for *(S)*-**13b**.

6-{4-[4-(2-Methoxyphenyl)piperazin-1-yl]butoxy}pyrazolo[1,5-*a*]pyridine-3-carbaldehyde (14a). To a solution of **12a** (54.4 mg, 0.143 mmol) in dry DMF (0.46 mL) was added POCl3 (40 µL, 0.443 mmol). After stirring at room temperature for 1 h, the reaction was quenched by addition of ice cold water and alkalized by addition of 5 M NaOH. The mixture was extracted twice with $CHCl_3$ and the combined organic layers were dried (Na_2SO_4). After evaporation, the crude product was purified by column chromatography (dichloromethane/methanol 98:2 to 95:5) to afford **14a** as orange solid (46.3 mg, 79%). Mp: 87 °C. IR (NaCl): 3099, 2943, 2816, 1663, 1519, 1278, 1241, 1185, 748 cm^{-1}. ^1H NMR ($CDCl_3$, 600 MHz, δ): 1.71–1.79 (m, 2 H), 1.87–1.95 (m, 2 H), 2.50 (t, *J* = 7.6 Hz, 2 H), 2.66–2.70 (m, 4 H), 3.09–3.14 (m, 4 H), 3.86 (s, 3 H), 4.05 (t, *J* = 6.4 Hz, 2 H), 6.86 (dd, *J* = 8.0 Hz, 1.3 Hz, 1 H), 6.89–6.96 (m, 2 H), 7.00 (ddd, *J* = 8.0 Hz, 6.6 Hz, 2.5 Hz, 1 H), 7.30 (dd, *J* = 9.7 Hz, 2.2 Hz, 1 H), 8.15–8.18 (m, 2 H), 8.28 (s, 1 H), 9.98 (s, 1 H). ^{13}C NMR ($CDCl_3$, 90 MHz, δ): 23.3, 27.1, 50.7, 53.5, 55.4, 58.2, 69.1, 111.3, 112.7, 113.8, 118.2, 119.0, 121.0, 122.9, 123.7, 135.5, 141.4, 146.2, 150.6, 152.3, 183.1. ESI-MS: *m/z* 409 [$M+H^+$]. Anal. calcd (%) for $C_{23}H_{28}N_4O_3$ x 0.3 H_2O: C 66.74, H 6.97, N 13.54; found: C 66.39, H 6.76, N 13.89.

5-{4-[4-(2-Methoxyphenyl)piperazin-1-yl]butoxy}pyrazolo[1,5-*a*]pyridine-3-carbaldehyde (14b). Compound **14b** was prepared according to the protocol of **14a** employing a solution of **12b** (800 mg, 2.11 mmol) in dry DMF (6.74 mL) and $POCl_3$ (0.61 mL). Purification by column chromatography (dichloromethane/methanol 98:2 to 95:5) afforded **14b** as off-white solid (840 mg, 98%) Mp: 90 °C. IR (NaCl) 2941, 2816, 1663, 1527, 1275, 1241, 1194, 772 cm^{-1}. ^1H NMR ($CDCl_3$, 600 MHz, δ): 1.72–1.77 (m, 2 H), 1.89–1.93 (m, 2 H), 2.50 (t, *J* = 7.6 Hz, 2 H), 2.67–2.70 (m, 4 H), 3.09–3.13 (m, 4 H), 3.86 (s, 3 H), 4.15 (t, *J* = 6.3 Hz, 2 H), 6.71 (dd, *J* = 7.6 Hz, 2.6 Hz, 1 H), 6.86 (dd, *J* = 7.9 Hz, 1.0 Hz, 1 H), 6.92 (ddd, *J* = 7.5 Hz, 7.0 Hz, 1.0 Hz, 1 H), 6.95 (dd, *J* = 7.5 Hz, 1.7 Hz, 1 H), 6.99 (ddd, *J* = 7.9 Hz, 7.0 Hz, 1.7 Hz, 1 H), 7.57 (d, *J* = 2.6 Hz, 1 H), 8.26 (s, 1 H), 8.37 (d, *J* = 7.6 Hz, 1 H),

9.94 (s, 1 H). ^{13}C NMR ($CDCl_3$, 90 MHz, δ): 23.4, 26.9, 50.7, 53.5, 55.4, 58.2, 69.0, 97.8, 109.6, 111.3, 113.3, 118.3, 121.1, 123.0, 130.1, 141.4, 141.6, 147.5, 152.3, 160.7, 183.1. HR-EIMS: [M^+] calcd for $C_{23}H_{28}N_4O_3$, 408.2161; found 408.2164. Anal. calcd (%) for $C_{23}H_{28}N_4O_3$ x 0.3 H_2O: C 66.74, H 6.97, N 13.54; found: C 66.62, H 6.79, N 13.52.

(*S*)-6-{4-[(5-Hydroxy-1,2,3,4-tetrahydronaphthalen-2-yl)(propyl)amino]butoxy} pyrazolo[1,5-*a*]pyridine-3-carbaldehyde (*(S)*-15a). Compound *(S)*-**13a** (40 mg, 0.10 mmol) was dissolved in 2 mL dry DMF, before $POCl_3$ (28 µL, 0.30 mmol) was added and the reaction mixture was stirred for 1 h in room temperature. Then the reaction mixture was cooled down to 0 °C and quenched with water, alkylized with 5M NaOH solution and extracted three times with dichloromethane. The organic layer was dried over anhydrous Na_2SO_4 and evaporated in vacuo. Column chromatographic purification using ethyl acetate and methanol (8:2) yielded 35 mg (82%) of *(S)*-**15a** as colourless oil. ^{1}H NMR (600 MHz, CD_3OD, δ): 0.93 (t, *J* = 7.4 Hz, 3 H), 1.51–1.62 (m, 3 H), 1.70–1.75 (m, 2 H), 1.86–1.90 (m, 2 H), 2.09–2.12 (m, 1 H), 2.47–2.52 (m, 1 H), 2.59–2.62 (m, 2 H), 2.71–2.77 (m, 3 H), 2.82–2.86 (m, 1 H), 2.94–3.00 (m, 2 H), 4.08–4.12 (m, 2 H), 6.53 (d, *J* = 7.5 Hz, 2 H), 6.87 (t, *J* = 7.4 Hz, 1 H), 7.42 (dd, *J* = 2.2, 9.5 Hz, 1 H), 8.11 (d, *J* = 9.3 Hz, 1 H), 8.40 (d, *J* = 2.2 Hz, 1 H), 8.41 (s, 1 H), 9.89 (s, 1 H). ^{13}C NMR (150 MHz, CD_3OD, δ): 12.2, 22.4, 24.7, 25.6, 26.6, 28.1, 32.9, 51.3, 58.4, 61.7, 70.4, 112.7, 114.4, 114.9, 119.6, 121.5, 124.3, 125.4, 127.3, 136.7, 138.4, 147.7, 152.3, 155.9, 185.2. HPLC (system 1) t_R = 14.0 min, purity 95%. $[\alpha]_{589}$ = -26.7° (28.4 °C, c 0.51, MeOH). ESI-MS: *m/z* 422.9 [$M+H^+$]. HRMS-ESI: [$M+H^+$] calcd for $C_{25}H_{32}N_3O_3$, 422.2438; found 422.2433.

(*S*)-5-{4-[(5-Hydroxy-1,2,3,4-tetrahydronaphthalen-2-yl)(propyl)amino]butoxy} pyrazolo[1,5-*a*]pyridine-3-carbaldehyde (*(S)*-15b). Compound *(S)*-**13b** (46 mg, 0.12 mmol) was dissolved in 2 mL dry DMF, before $POCl_3$ (32 µL, 0.35 mmol) was added and the reaction mixture was stirred for 1 h at room temperature. Then the reaction mixture was cooled down to 0 °C and quenched with water and alkylated with 5M NaOH solution and

extracted three times with dichloromethane. The organic layer was dried over anhydrous Na_2SO_4 and evaporated in vacuo. Column chromatographic purification using ethyl acetate and methanol (8:2) yielded 41 mg (83%) of *(S)*-**15b** as colourless oil. ^{1}H NMR (CD_3OD, 600 MHz, δ): 1.00 (t, *J* = 7.2 Hz, 3 H), 1.69 (sextet, *J* = 7.5 Hz, 2 H), 1.73–1.79 (m, 1 H), 1.85–1.90 (m, 2 H), 1.94–1.98 (m, 2 H), 2.21–2.24 (m, 1 H), 2.55–2.61 (m, 1 H), 2.89–2.94 (m, 3 H), 2.97–3.06 (m, 4 H), 3.34–3.38 (m, 1 H), 4.24 (t, *J* = 6.2 Hz, 2 H), 6.58 (bd, *J* = 8.2 Hz, 2 H), 6.86 (dd, *J* = 2.9, 7.4 Hz, 1 H), 6.93 (t, *J* = 7.7 Hz, 1 H), 7.62 (d, *J* = 2.8 Hz, 1 H), 8.41 (s, 1 H), 8.56 (d, *J* = 7.6 Hz, 1 H), 9.87 (s, 1 H). ^{13}C NMR (CD_3OD, 150 MHz, δ): 11.8, 21.2, 24.3, 24.4, 25.8, 27.5, 31.4, 51.6, 53.8, 60.0, 69.7, 98.6, 110.7, 113.1, 114.3, 121.4, 123.7, 127.7, 131.9, 142.9, 148.9, 156.1, 162.5, 185.3. HPLC (system 1) t_R = 14.0 min, purity 99%. $[\alpha]_{589}$ = -22.5° (28 °C, c 0.48, MeOH) ESI-MS: *m/z* 422.9 [M+H$^+$]. HRMS-ESI: [M+H$^+$] calcd for $C_{25}H_{32}N_3O_3$, 422.2438; found 422.2428.

6-{4-[4-(2-Methoxyphenyl)piperazin-1-yl]butoxy}lpyrazolo[1,5-*a*]pyridine-3-carbaldehydoxime (16a). Title compound **16a** was prepared according to the protocol of **12f** employing a solution of **14a** (35 mg, 0.08 mmol) and hydroxylamine hydrochloride (12 mg, 0.16 mmol). Preparative HPLC purification of the crude product under conditions of method A (t_R = 15.9 min), yielded **16a** as white solid (30 mg, 70%). ^{1}H NMR (600 MHz, CD_3OD, δ): 1.95–1.99 (m, 2 H), 2.01–2.06 (m, 2 H), 3.05 (t, *J* = 12.3 Hz, 2 H), 3.29–3.35 (m, 4 H), 3.61 (d, *J* = 13.2 Hz, 2 H), 3.68 (d, *J* = 12.3 Hz, 2 H), 3.87 (s, 3 H), 4.14 (t, *J* = 5.9 Hz, 2 H), 6.93 (dt, *J* = 6.9, 1.3 Hz, 1 H), 7.00 (dd, *J* = 7.8, 1.3 Hz, 2 H), 7.07–7.09 (m, 1 H), 7.23 (d, J = 9.4 Hz, 1 H), 7.72 (bs, 1 H), 7.91 (d, J = 9.4 Hz, 1 H), 9.38 (s, 1 H), 8.67 (s, 1 H). ^{13}C NMR ($CDCl_3$, 150 MHz, δ): 20.8, 26.2, 26.3, 47.7, 52.2, 55.4, 56.7, 56.8, 67.8, 68.0, 111.3, 112.7, 118.9, 120.5, 120.7, 121.2, 123.4, 124.6, 138.8, 148.9, 150.1, 152.08. HPLC (system 1) t_R = 12.1 min, purity 95%. ESI-MS: *m/z* 424.7 [M+H$^+$]. HRMS-ESI: [M+H$^+$] calcd for $C_{23}H_{30}N_5O_3$, 424.2343; found 424.2341.

5-{4-[4-(2-Methoxyphenyl)piperazin-1-yl]butoxy}lpyrazolo[1,5-*a*]pyridine-3-carbaldehydoxime (16b, 16c) Compounds **16b** and **16c** were prepared according to the protocol of **12f** employing a solution of hydroxylamine hydrochloride (30.1 mg, 0.433 mmol) in distilled water (1.2 mL) and 2 M NaOH (0.11 mL, 0.22 mmol), as well as a solution of **14b** (88.4 mg, 0.217 mmol) in ethanol (10.9 mL). Purification of the crude product by column chromatography (dichloromethane/methanol 98:2 to 95:5) separately afforded the *s-trans* isomer **16b** (42 mg, 46%) and the *s-cis* isomer **16c** (39 mg, 43%) in a 1:1 ratio. Analytical data for **16b**: Mp: 77 °C. IR (NaCl): 3257, 3064, 2945, 2823, 1647, 1541, 1269, 1242, 1026, 750 cm^{-1}. ^{1}H NMR ($CDCl_3$, 360 MHz, δ): 1.78–1.83 (m, 2 H), 1.86–1.90 (m, 2 H), 2.55 (t, *J* = 7.6 Hz, 2 H), 2.71–2.77 (m, 4 H), 3.14–3.20 (m, 4 H), 3.87 (s, 3 H), 4.05 (t, *J* = 6.3 Hz, 2 H), 6.45 (dd, *J* = 7.6 Hz, 2.6 Hz, 1 H), 6.86 (dd, *J* = 7.9 Hz, 1.0 Hz, 1 H), 6.91 (ddd, *J* = 7.5 Hz, 7.0 Hz, 1.0 Hz, 1 H), 6.96 (dd, *J* = 7.5 Hz, 2.0 Hz, 1 H), 7.00 (ddd, *J* = 7.9 Hz, 7.0 Hz, 2.0 Hz, 1 H), 7.20 (d, *J* = 2.6 Hz, 1 H). 7.93 (s, 1 H), 8.22 (d, *J* = 7.6 Hz, 1 H), 8.27 (s, 1 H), free OH n. d. ^{13}C NMR ($CDCl_3$, 90 MHz, δ): 23.3, 27.0, 50.4, 53.4, 55.4, 58.3, 68.3, 97.2, 103.7, 107.9, 111.2, 118. 4, 121.1, 123.1, 129.5, 138.6, 141.1, 143.3, 143.6, 152.3, 157.6. ESI-MS: 423 [M^+]. Anal. calcd (%) for $C_{23}H_{29}N_5O_3$ x 0.5 H_2O: C 63.87, H 6.99, N 16.19; found: C 63.88, H 6.88, N 16.02. Analytical data for **16c**: Mp: 138 °C. IR (NaCl): 3324, 2945, 2821, 1647, 1541, 1238, 1026, 750 cm^{-1}. ^{1}H NMR ($CDCl_3$, 600 MHz, δ): 1.74–1.82 (m, 2 H), 1.87–1.94 (m, 2 H), 2.54 (t, *J* = 7.6 Hz, 2 H), 2.70–2.75 (m, 4 H), 3.12–3.18 (m, 4 H), 3.87 (s, 3 H), 4.08 (t, *J* = 6.3 Hz, 2 H), 6.54 (dd, *J* = 7.6 Hz, 2.6 Hz, 1 H), 6.86 (dd, *J* = 7.9 Hz, 1.0 Hz, 1 H), 6.88–7.02 (m, 4 H), 7.50 (s, 1 H), 8.30 (d, *J* = 7.6 Hz, 1 H), 8.67 (s, 1 H), free OH n. d. ^{13}C NMR ($CDCl_3$, 90 MHz, δ): 23.3, 26.9, 50.5, 53.5, 55.4, 58.1, 68.4, 94.4, 102.4, 107.7, 111.3, 118.3, 121.1, 123.0, 129.9, 137.9, 140.5, 141.3, 146.2, 152.3, 157.6. ESI-MS: 423 [M^+]. Anal. calcd (%) for $C_{23}H_{29}N_5O_3$ x 0.7 H_2O: C 63.34, H 7.03, N 16.06; found: C 63.21, H 6.77, N 15.90.

(*S*)-6-{4-[(5-Hydroxy-1,2,3,4-tetrahydronaphthalen-2-yl)(propyl)amino]butoxy} pyrazolo[1,5-*a*]pyridine-3-carbaldehyde oxime (*(S)*-17a). Title compound *(S)*-**17a** was prepared according to the synthesis of **12f**, employing *(S)*-**15a** (19 mg, 0.04 mmol) and hydroxylamine hydrochloride (6 mg, 0.10 mmol). Column chromatographic purification (ethyl acetate/methanol 95:5) yielded *(S)*-**17a** as colorless oil (15 mg, 76%). ^{1}H NMR ($CDCl_3$, 600 MHz, δ): 0.95 (t, *J* = 7.3 Hz, 3 H), 1.57–1.68 (m, 3 H), 1.74–1.80 (m, 2 H), 1.86–1.91 (m, 2 H), 2.14–2.17 (m, 1 H), 2.50–2.56 (m, 1 H), 2.71–2.74 (m, 2 H), 2.79–2.85 (m, 3 H), 2.88–2.92 (m, 1 H), 2.97–3.01 (m, 1 H), 3.11–3.15 (m, 1 H), 4.07 (q, *J* = 6.0 Hz, 2 H), 6.53 (dd, *J* = 3.0, 7.6 Hz, 0.15 H), 6.56 (d, *J* = 7.7 Hz, 2 H), 6.89 (t, *J* = 7.7 Hz, 1 H), 6.94 (d, *J* = 2.7 Hz, 0.15 H), 7.13 (dd, *J* = 2.2, 9.6 Hz, 0.4 H), 7.17 (dd, *J* = 2.2, 9.6 Hz, 0.4 H), 7.60 (s, 0.4 H), 7.82 (d, *J* = 2.7 Hz, 0.15 H), 7.83 (d, *J* = 9.8 Hz, 0.4 H), 7.92 (d, *J* = 9.8 Hz, 0.4 H), 7.98 (s, 0.4 H), 8.19 (d, *J* = 2.0 Hz, 0.4 H), 8.21 (d, *J* = 2.0 Hz, 0.4 H), 8.24 (s, 0.4 H), 8.30 (d, *J* = 8.0 Hz, 0.15 H), 8.63 (s, 0.4 H). ^{13}C NMR (CD_3OD, 150 MHz, δ): 12.1, 14.5, 20.9, 21.9, 24.6, 25.2, 26.3, 27.9, 28.0, 32.6, 51.5, 53.8, 59.1, 61.6, 69.9, 70.0, 96.8, 106.9, 108.5, 112.9, 113.0, 113.1, 117.9, 120.2, 121.5, 124.1, 127.5, 134.9, 136.7, 137.7, 142.0, 143.5, 145.2, 151.1, 156.0. HPLC (system 1) t_R = 14.1 min, purity 96 %. ESI-MS: *m/z* 437.9 [M+H$^+$]. HRMS-ESI: [M+H$^+$] calcd for $C_{25}H_{33}N_4O_3$, 437.2547; found 437.2546.

(*S*)-5-{4-[(5-Hydroxy-1,2,3,4-tetrahydronaphthalen-2-yl)(propyl)amino]butoxy} pyrazolo[1,5-*a*]pyridine-3-carbaldehyde oxime (*(S)*-17b). Title compound *(S)*-**17b** was prepared according to the protocol of **12f**, employing *(S)*-**15b** (41 mg, 0.10 mmol) and hydroxylamine hydrochloride (13 mg, 0.20 mmol). Column chromatographic purification (ethyl acetate) yielded *(S)*-**17b** as colorless oil (15 mg, 35%). ^{1}H NMR ($CDCl_3$, 600 MHz, δ): 0.93 (t, *J* = 7.4 Hz, 3 H), 1.55–1.59 (m, 2 H), 1.63–1.75 (m, 3 H), 1.81–1.88 (m, 2 H), 2.14–2.18 (m 1 H), 2.55–2.61 (m, 3 H), 2.69–2.71 (m, 2 H), 2.79–2.84 (m, 1 H), 2.90–2.92 (m, 1 H), 2.95–3.00 (m, 1 H), 3.06–3.10 (m, 1 H), 3.99–4.03 (m, 2 H), 6.51 (dd, *J* = 2.7, 7.4 Hz, 1 H), 6.63 (d, *J* = 7.4 Hz, 1 H), 6.67 (d, *J* = 7.4 Hz, 1 H), 6.98 (t, *J* = 7.4 Hz, 1 H), 7.22 (d, *J* =

2.8 Hz, 1 H), 7.94 (s, 1 H), 8.27 (d, *J* = 7.7 Hz, 1 H), 8.29 (s, 1 H). ^{13}C NMR ($CDCl_3$), 90 MHz, δ): 11.9, 14.2, 21.0, 23.6, 25.3, 26.8, 31.4, 50.1, 52.4, 60.4, 68.4, 97.3, 103.5, 108.0, 112.1, 121.7, 122.9, 126.5, 129.6, 137.9, 138.7, 143.4, 144.0, 153.6, 157.4. HPLC (system 1) t_R = 13.7 min, purity 98%. ESI-MS: *m/z* 437.9 [M+H$^+$]. HRMS-ESI: [M+H$^+$] calcd for $C_{25}H_{33}N_4O_3$, 437.2547; found 437.2549.

5-{4-[4-(2-Methoxyphenyl)piperazin-1-yl]butoxy}lpyrazolo[1,5-*a*]pyridine-3-carbonitrile (18). A solution of **16b**/**c** (40.1 mg, 0.095 mmol) in acetic acid anhydride (0.47 mL) was refluxed for 7 h. After cooling, the reaction mixture was diluted with ice cold water and extracted with CH_2Cl_2. The combined organic layers were dried (Na_2SO_4) and evaporated in vacuo. Purification by column chromatography (dichloromethane/methanol 98:2 to 95:5) afforded **18** as white solid (31 mg, 79%) Mp: 92 °C. IR (NaCl) 3070, 2937, 2816, 2219, 1648, 1542, 1240, 1028, 749 cm^{-1}. ^{1}H NMR ($CDCl_3$, 360 MHz, δ): 1.71–1.80 (m, 2 H), 1.88–1.96 (m, 2 H), 2.52 (t, *J* = 8.0 Hz, 2 H), 2.68–2.72 (m, 4 H), 3.10–3.14 (m, 4 H), 3.86 (s, 3 H), 4.11 (t, *J* = 6.1 Hz, 2 H), 6.66 (dd, *J* = 7.6 Hz, 2.6 Hz, 1 H), 6.86 (dd, *J* = 7.8 Hz, 1.4 Hz, 1 H), 6.91–6.96 (m, 3 H), 7.02 (ddd, *J* = 7.8 Hz, 6.8 Hz, 2.5 Hz, 1 H), 8.10 (s, 1 H), 8.34 (d, *J* = 7.6 Hz, 1 H). ^{13}C NMR ($CDCl_3$, 90 MHz, δ) 23.3, 26.9, 50.6, 53.5, 55.4, 58.1, 69.0, 80.9, 95.0, 109.3, 111.3, 114.5, 118.3, 121.1, 123.0, 130.5, 141.4, 144.4, 145.6, 152.4, 159.3. HPLC (system 1): t_R = 14.9 min, purity > 99 %. HR-EIMS: [M$^+$] calcd for $C_{23}H_{27}N_5O_2$, 405.2165; found 405.2168.

Membrane preparations. Membranes were obtained using a previously described protocol.[75] Briefly, HEK293T cells were grown to a confluence of 70 % and transiently transfected with the receptor of interest with or without co-transfection of a PTX insensitive Gα subunit using the Mirus TransIT-293 transfection reagent (MoBiTec, Goettingen, Germany) or $CaHPO_4$ precipitation. 48 h after transfection, cells were washed with ice cold phosphate buffered saline (PBS, pH 7.4) and detached with harvest buffer (10 mM Tris-HCl, 0.5 mM EDTA, 5.4 mM KCl, 140 mM NaCl, pH 7.4). After centrifugation (8 min, 220 *g*) the

pellet was resuspended in 10 mL ice cold homogenate buffer (50 mM Tris-HCl, 5 mM EDTA, 1.5 mM $CaCl_2$ 5 mM $MgCl_2$, 5 mM KCl, 120 mM NaCl, pH 7.4) and cells were lysed with an ultraturrax. After ultracentrifugation (30 min, 50,000 *g*), membranes were resuspended in binding buffer (50 mM Tris-HCl, 1 mM EDTA, 5 mM $MgCl_2$, 100 µg/mL bacitracin, 5 µg/mL soybean trypsin inhibitor, pH 7.4) and homogenized with a glass-Teflon homogenizer at 4°C. Membrane preparations were shock-frozen in liquid nitrogen and stored at -80 °C. The protein concentration was determined with the method of Lowry[76] applying bovine serum albumin as standard. Membranes from stably transfected CHO cells were obtained in an analogous manner.

Competition binding experiments. Receptor binding studies were carried out as described previously.[77] Briefly, for competition binding experiments with the human D_{2L},R, $D_{2S}R$, D_3R and D_4R, preparations of membranes from CHO cells stably expressing the corresponding receptors were used together with [^{3}H]spiperone (specific activity of 81 Ci/mmol, PerkinElmer, Rodgau, Germany) at a final concentration of 0.10–0.30 nM (K_D 0.03-0.085, 0.085-0.18, 0.03-0.095 and 0.13-0.29 nM, respectively). Competition binding experiments with the human D_1R and 5-$HT_{2A}R$ were performed in an analogous manner with membranes from transiently transfected HEK293T cells together with [^{3}H]SCH23990 (60 Ci/mmol, Biotrend, Cologne, Germany, final concentration 0.40-0.50 nM, K_D 0.32-0.48 nM) or [^{3}H]ketanserin (53 Ci/mmol, PerkinElmer, final concentration 0.20-0.50 nM, K_D 0.19-0.40 nM), respectively. Binding studies with porcine α_1R or 5-$HT_{1A}R$ were carried out as described previously wit homogenates from porcine cerebral cortex,[77] in the presence of the radioligands [^{3}H]prazosin (83 Ci/mmol, PerkinElmer, 0.10-0.20 nM final concentration, K_D 0.040-0.087 nM) or [^{3}H]WAY100635 (80 Ci/mmol, Biotrend, 0.30 nM final concentration, K_D 0.030-0.060 nM). Resulting competition curves were analyzed by nonlinear regression using the algorithms in PRISM 6.0 (GraphPad software, San Diego, CA). The data

were fit using a sigmoid model to provide an IC_{50} value which was transformed into a K_i value employing the equation of Cheng and Prusoff.[78]

[^{35}S]GTPγS binding experiments. [^{35}S]GTPγS incorporation assays were performed as described previously.[10] Membranes from HEK293T cells transiently transfected with $D_{2S}R$ or D_3R and G protein subunits $G\alpha_{oA}$ or $G\alpha_{i2}$ (protein concentration 30 µg/mL) were incubated with 10 µM GDP and the test compounds in incubation buffer (20mM HEPES, 10 mM $MgCl_2$•6 H_2O, 100 mM NMDG and 70 mg/L saponin) for 30 min at 37°C in a final volume of 200µL. After the addition of 0.1 nM [^{35}S]GTPγS (1250 Ci/mmol, PerkinElmer) incubation was continued for another 75 min at 37 °C (30 min for D_{2S} + $G\alpha_{oA}$). The reaction was terminated by filtration through Whatman GF/B filters soaked with ice cold PBS. Bound radioactivity was measured as described previously.[75] Four to six experiments per compound were performed with each concentration (0.1 pM to 10 µM) in triplicate. Dose response curves were analyzed using the algorithms for non-linear regression in Prism 6.0. All responses were normalized to the reference agonist quinpirole (100%) and buffer conditions (0%).

PathHunter assay. $D_{2S}R$ mediated β-arrestin-2 recruitment was determined using the PathHunter assay (DiscoveRx, Birmingham, U.K.) as described previously.[10] In brief, HEK293 cells stably expressing the enzyme acceptor (EA) tagged β-arrestin-2 fusion protein were transiently transfected with the ProLink tagged $D_{2S}R$-ARMS2-PK2 construct employing Mirus TransIT-293. 24 h after transfection, cells were detached from the culture dish with Versene (Life Technologies, Darmstadt, Germany), seeded into 384-well plates (5000 cells/well) and maintained for 24 h at 37 °C, 5 % CO_2. After incubation with the test compounds dissolved in PBS for 5 h at 37 °C, the detection mix was added and incubation was continued for further 60 min at room temperature. Chemiluminescence was determined using the Victor^3-V plate reader (PerkinElmer, Rodgau, Germany). Three to eight experiments per compound were performed, with each concentration in duplicate. All

responses were normalized to the effect of 10 μM quinpirole (100%) and buffer conditions (0%).

Bioluminescence resonance energy transfer. D_{2S}, D_{2L} and D_3 receptor mediated activation of $G\alpha_{i/o}$ proteins was determined employing BRET²-biosensors based on the separation of RLucII-Gα and Gβγ-GFP10 as previously described.[39-42] Recruitment of RLucII-β-arrestin-1 and RLucII-β-arrestin-2 was determined employing a recently described protocol based on bystander BRET with CAAX-rGFP.[48] Briefly, HEK293 cells were seeded into 12-well plates (1.2 mL/2.4 x 10^5 cells/mL) in DMEM supplemented with 10 % FBS, 100 μg/mL penicillin, 100 μg/mL streptomycin and transfected using a solution of polyethylenimine in PBS (PEI, linear 25 kDa, Polysciences, 1 mg/mL) as transfection reagent at a 3:1 PEI to cDNA ratio. Cells were simultaneously transfected with N-terminal FLAG-tagged $D_{2L}R$, $D_{2S}R$, or D_3R, RLucII-$G\alpha_{i1-3}$ or RLucII-$G\alpha_{oA/B}$, $G\beta_1$ and $G\gamma_2$-GFP10, or FLAG-tagged $D_{2L}R$, $D_{2S}R$, RLucII- β-arrestin-1 or RLucII- β-arrestin--2 and CAAX-rGFP, respectively. The total amount of cDNA was kept at 1 μg cDNA/well by addition of single stranded salmon sperm DNA (Sigma Aldrich). Transfected cells were transferred to white 96-well plates (100 μL/well, Greiner, Frickenhausen, Germany) pretreated with poly-D-lysine (0.1 mg/mL, MP-Biomedicals, Illkirch, France) and incubated at 37°C, 5 % CO_2. 48h after transfection, cells were rinsed with PBS twice and incubated with 90 μL tyrode's buffer (137 mM NaCl, 0.9 mM KCl, 1 mM $MgCl_2$•6 H_2O, 1 mM $CaCl_2$, 11.9 mM NaH_2PO_4, 5.5 mM D-glucose, 3.6 mM $NaHCO_3$, 25 mM HEPES, pH 7.4) at 37°C for 1-2 h. For each combination of biosensors, BRET titration experiments were performed to determine optimal donor/acceptor cDNA ratios.[40] A constant amount of RlucII-tagged donor cDNA was co-expressed with increasing amounts of GFP10- or rGFP-tagged acceptor cDNA, respectively. GFP-fluorescence was determined on a FLEX-stationII (Perkin Elmer) with an excitation wavelength of 400 nm and emission wavelength at 515 nm for GFP10, or 480 nm and 538 nm for rGFP. For G protein activation, cells were incubated with 10 μM dopamine or vehicle for

10 min at 37 °C. For β-arrestin recruitment, incubation time was increased to 15 min. Coelenterazine 400a (DBC™, 2.5 μM final concentration), was added 5 min before the BRET measurement. BRET readings were obtained on a NeoSynergy (Bio-tek Instruments, Bad Friedrichshall, Germany) with the respective filter set (donor 410 ± 80 nm and acceptor 515 ± 30 nm) as ratio of the light emitted by the acceptor (GFP10 or rGFP) divided by signal from the light emitted by the donor (RLucII). Specific BRET (netBRET) was determined as difference of the observed absolute BRET and the BRET occurring in the absence of any fluorescent acceptor protein. Saturation curves were obtained in the absence and presence of 10 μM dopamine by plotting the specific BRET over the ratio of fluorescence (determined on FLEX-stationII) over luminescence determined at 410 nm. Data was analyzed using the algorithms for specific one-site binding in PRISM 6.0. Three independent experiments were performed, with each donor/acceptor ratio in quadruplicates. For dose-response curves, optimal transfection conditions were derived from the titration experiments. Ligand induced changes in BRET signal (ΔBRET) were calculated as difference between the BRET ratio obtained under vehicle conditions and the BRET ratio obtained with addition of ligands. Dose-response curves were fitted using the algorithms for three parameter non-linear regression in PRISM 6.0. Responses were normalized to the effect of 10 μM quinpirole (100%) and vehicle (0%). Three to eight experiments per compound were performed, with each concentration in duplicate.

Bias quantification. The operational model of agonism[43] was used to quantify ligand bias following recently published protocols.[45, 79] In brief, transduction ratios (τ/K_A) were obtained in their logarithmic form from data analysis with the algorithms implemented in PRISM6.0. Thus, normalized data for the activation of $G\alpha_{oA}$ (recorded by BRET) and the recruitment of β-arrestin-2 (determined in the PathHunter assay) were analyzed using the following equation:

$$Y = \text{basal} + \frac{(E_m - \text{basal})\left(\frac{\tau}{K_A}\right)^n [X]^n}{\left(\frac{\tau}{K_A}\right)^n [X]^n + \left(1 + \frac{[X]}{K_A}\right)^n}$$

with basal being the response of a the system in absence of an agonist, E_m the maximal response, [X] the concentration of the agonist and n the transducer slope. Parameters E_m and n were globally shared during the analysis, while basal was constrained to zero. Transduction coefficients (τ/K_A) were then normalized to the response of the reference agonist quinpirole to account for cell-system-dependent factors between different assay systems using:

$$\Delta \log\left(\frac{\tau}{K_A}\right) = log\left(\frac{\tau}{K_A}\right)_{test\ ligand} - log\left(\frac{\tau}{K_A}\right)_{reference\ ligand}$$

separately for each ligand and investigated signaling pathway. Determination of bias was performed by calculation of the difference for two investigated pathways for the same ligand:

$$\Delta\Delta \log\left(\frac{\tau}{K_A}\right)_{1,2} = \Delta log\left(\frac{\tau}{K_A}\right)_{signal\ 1} - \Delta\ log\left(\frac{\tau}{K_A}\right)_{signal\ 2}$$

$$bias\ factor = 10^{\Delta\Delta log\left(\frac{\tau}{K_A}\right)}$$

Standard errors were estimated as described previously[79] using the following equation:

$$SEM_{1,2} = \sqrt{{SEM_1}^2 + {SEM_2}^2}$$

Statistical significance was calculated using one-way ANOVA followed by Dunnett's posthoc test at the level of $\Delta\Delta\log(\tau/K_A)$ and accepting $p<0.05$ as level of significance.

Electrophysiological recordings. Activation of GIRK1/2 (Kir3.1/3.2) channels by $D_{2L}R$ or D_3R was assessed in analogy to a previously described protocol involving GIRK1/2 and $G\alpha_{i/o}$-coupled 5-$HT_{1A}R$.[59] 48 h before the experiment, HEK293T were transfected with the receptor of interest, a plasmid encoding GIRK1/2 and GFP employing Mirus TransIT-293. A total amount of 900 ng cDNA was used per culture dish (∅ 6 cm). On the day of the experiment, cells were detached using Versene and distributed into 35 mm dishes (BD Falcon) containing fresh medium (DMEM/F-12, 10% FBS, 100 µg/mL penicillin, 100 µg/mL

streptomycin and 0.5 mg/mL L-glutamine, Gibco, Life Technologies). Cells were allowed to attach for at least 30 min. Cells were washed twice with high K^+ bath solution (120 mM KCl, 5 mM NaCl, 2 mM $CaCl_2$, 2 mM $MgCl_2$, 5 mM HEPES, 10 mM Glucose, 50 mM Mannitol, pH 7.4, 315-330 mosmol/L) and covered with 2 mL of the bath solution for the recordings. All recordings were performed at room temperature (20 – 22 °C) in one-pipette whole-cell configuration and in voltage clamp mode. Transfected cells were identified by detection of the eGFP fluorescence under an inverted microscope. Recordings were sampled at 20 kHz and filtered at 5 kHz employing a Multiclamp 700B Amplifier and an Axon Digidata 1332A interface (Axon instruments, Molecular Devices, Biberach, Germany) with pClamp 10.3 or 10.4 software. Borosilicate capillaries were pulled to patch pipettes with a resistance of 2.5 – 3.5 MΩ when filled with internal solution (135 mM potassium gluconate, 2 mM NaCl, 3 mM $MgCl_2$, 5 mM HEPES, 5 mM EGTA, 0.3 mM Na GTP, 2 mM Na_2ATP, pH 7.2, 315-330 mosmol/L) employing a DMZ-Universal puller (Zeitz-Instruments, Martinsried, Germany). After obtaining the whole-cell configuration, access resistance was typically in the range of 2.5 – 5 MΩ before series resistance compensation (75%). Cells showed a typical capacitance of 10 – 20 pF. Recordings were started no earlier than three minutes after obtaining whole-cell access. Drugs were applied with a puff-pipette with a pressure of 1 bar. Puff-pipettes for the delivery of drugs were pulled under the same conditions used for the patch pipettes and were made from borosilicate capillaries with an internal filament. Antagonist solutions or the channel blocker Ba^{2+} (2 mM) were manually added to the bath solution. Recordings were either performed at a constant holding potential of -70 mV or with a voltage ramp from -120 mV to +60 mV executed within 1.1 s. Data analysis was performed using pClamp10.3 and PRISM 6.0. For the quantification of absolute currents, results from the voltage ramp protocols at the time point corresponding to -80 mV were used. Statistical analysis weas performed with PRISM 6.0 applying one-way analysis of variance (one-way ANOVA)

followed by a post hoc Tukey's test for multiple comparisons. Data are expressed as mean ± S.E.M. and $p < 0.05$ was accepted as level of significance.

Animal Studies. All experiments were carried out with the agreement of Animal Protection Law of the Federal Republic of Germany and the European Communities Council Directive of 24 November 1986 (86/609/EEC). Male Sprague-Dawley rats (Charles River, Germany) weighing 300-350 g at the beginning of the experiment were housed four animals per cage with food and water ad libitum. The housing room was maintained at 22±2 °C and a relative humidity of 55±10 %, under a 12 h/12 h light-dark cycle (lights on from 7am to 7pm). Experiments were carried out in the lights on phase, only. After handling and habituating the animals to the testing equipment, 44 animals were randomly divided into four groups, with three groups receiving intra peritoneal (i.p.) injections of escalating doses of D-amphetamine sulphate in 0.9 % saline (AMPH; 1ml/kg; Fagron, n=33) and the other group receiving i.p. injections of 0.9 % saline (SAL; 1ml/kg, n=11) three times per day (9am; 1pm and 5 pm) for six days. The concentration of AMPH was increased from 1 mg/kg to 8 mg/kg during the first eight injections and sustained at 8mg/kg for the following ten injections.[62] **1a** (Sigma Aldrich, Germany, 1.5 mg/kg/day) and **16c** (1.5 mg/kg/day) were dissolved in a 2% glacial acetic acid/H_2O with 25% DMSO. Drugs or vehicle (VEH, glacial acetic acid/H_2O, 25% DMSO) were administered via an Alzet osmotic mini pump (model 2ML1; 7 day delivery; DURECT Corporation). Alzet pumps were implanted one day after the last AMPH or SAL injection under isoflurane (Baxter Germany GMBH; 5% induction, 2% maintenance) anesthesia mixed with oxygen, which was administered by a nose cone. A small skin incision was made on the lower back of each animal and a small pocket was formed by loosening the subcutaneous connective tissues with a hemostat. The pump was inserted with the flow moderator pointing away from the incision. The incision was closed using surgical staples, and disinfected with aluminum spray.[80] SAL-injected animals received VEH treatment, and the AMPH-injected animals received VEH, **1a** (1.5mg/kg/day), or **16c** (1.5mg/kg/day) treatment, which resulted

in four treatment groups: SAL/VEH (n=11), AMPH/VEH (n=12), AMPH/**1a** (n=12), and AMPH/**16c** (n=9).

Amphetamine-induced hyperactivity. AMPH-induced hyperlocomotion was tested in an open field (OF). Animals were allowed to freely explore a cubic gray acrylic arena with the dimensions of 50 x 50 x 50 cm with evenly distributed 25 lux white light. The central zone was defined as a square that resided in the center of the box with the dimensions of 25 x 25 cm. The activities of the animals were recorded by video and analyzed using Biobserve Viewer III (Biobserve GMBH, Germany). The horizontal locomotion and central zone duration were measured using Biobserve Viewer III software, whereas the vertical activity was determined manually. When an animal raised both of its front legs, this activity was considered as a vertical activity. Each parameter was measured in blocks of 5 min. Animals were allowed to habituate twice to an OF apparatus in 20 min sessions before the AMPH-sensitization procedure. Seven days after the mini pump implantation, animals were tested in the OF. First, the baseline activity of the animals was assessed for 20 min. After this period, each animal was i.p. injected with 1.5 mg/kg AMPH, and their locomotor activities and anxiety-related behaviors were measured for 20 min. AMPH-induced effects were normalized to the activity during the last 5 min of the baseline period. The AMPH-induced activity was calculated as delta (Δ) from this baseline interval.

Light- induced activity (LIA). Five days after the mini pump implantation, the light-induced activity test was conducted to determine horizontal and vertical activities of animals induced by a white light stimulus. Therefore, a commercialized TruScan system arena (Coulbourn Instruments, Allentown, USA) was used for to measure the behavioral activity by a light beam system within a 40 x 40 x 39 cm open field box, which was situated in a sound- and light-isolated room. The horizontal activity was measured by the number of interruptions of the two-dimensional (X and Y) beams (located 3 cm above the floor of the box) detected automatically by a computer. The vertical activity was measured by the disruptions of the

light beams located 12 cm above the floor of the test box. The test boxes were illuminated by 2.6 lux red light throughout the experimental session. A fluorescent lamp (16W, 82 lux), which was mounted on the top of the test box, was used for white light stimulation.[64, 66] For the first 20 min, animals were habituated to the test box in the absence of light induction. This baseline period was followed by a 20 min test session, in which 10 randomly distributed light stimuli (82 lux) with 30 sec duration were presented according to the protocol used in previous studies.[64] Horizontal and vertical activities were automatically measured by the TruScan system. Light-induced effects were normalized to the activity in the last 5 min of habituation period. The subsequent light-induced activity was calculated as Δ from this baseline interval.

Statistical analysis. Data from behavioral experiments was analyzed as mean ± SEM. All the experiments were analyzed by a two-way ANOVA with the factors treatment and time. Pre-planned analyses were calculated to compare group differences using Bonferroni-corrected LSD tests. Differences were calculated as both overall activity and activity at single time points. For LIA analyses, two-tailed t tests were conducted. Statistical significance was set $p < 0.05$ for all tests. All statistical analyses were carried out with IBM SPSS 21 software (SPSS Inc., Chicago, Illinois).

ASSOCIATED CONTENT

Supporting Information. Supplementary Figures, supplementary results of functional assays and *in vivo* characterization, ^{1}H and ^{13}C NMR spectra. This material is available free of charge via the Internet at http://pubs.acs.org.

AUTHOR INFORMATION

Corresponding Author. *To whom correspondence should be addressed. Mailing address: Department of Chemistry and Pharmacy, Emil Fischer Center, Friedrich Alexander University, Schuhstr. 19, 91052 Erlangen, Germany. Tel: +49 9131 85-29383. Fax: +49 9131 85-22585. Email: peter.gmeiner@fau.de.

ACKNOWLEDGMENTS

This work was supported by the Deutsche Forschungsgemeinschaft (DFG) grants GRK1910 and MU 2789/7-1 and by a grant from the Canadian Institute for Health Research (CIHR) # 11215 to MB. MB holds a Canada research chair in signal transduction and Molecular Pharmacology. We thank Dr. Monique Lagacé (IRIC, University of Montreal, Canada) for help with the BRET experiments and helpful discussions. We thank Prof. Graeme Milligan (University of Glasgow, U.K.) for providing us with the cDNA for $G\alpha_{oA}$ and $G\alpha_{i2}$ proteins.

ABBREVIATIONS USED

AMPH, amphetamine; APCI, atmospheric pressure chemical ionization; BRET, bioluminescence resonance energy transfer; CHO, chinese hamster ovary; 1,4-DAP, 1,4-disubstituted-aromatic piperazine; D_xR, dopamine D_x receptor; $G\alpha_x$, G protein subunit $G\alpha_x$; GFP10, green fluorescent protein variant; rGFP, Renilla reniformis green fluorescent protein; GIRK, G protein-coupled inward rectifying potassium channel, GTPγS, guanosine 5'-*O*-(thiotriphosphate); HATU, (1-[Bis(dimethylamino)methylene]-1*H*-1,2,3-triazolo[4,5-*b*]pyridinium 3-oxid hexafluorophosphate); hD_xR, human dopamine D_x receptor; $h5\text{-}HT_xR$, human serotonin $5\text{-}HT_x$ receptor; LIA, light induced activity; $p\alpha_xR$, porcine adrenergic α_x receptor; $p5\text{-}HT_xR$, porcine serotonin $5\text{-}HT_x$ receptor; PPI, prepulse inhibition; PTX, pertussis

toxin; RLucII; Renilla luciferase; SAL, saline; S.D., standard deviation; S.E.M, standard error of mean; TM, transmembrane helix; VEH, vehicle.

REFERENCES

1. Welsch, M. E.; Snyder, S. A.; Stockwell, B. R. Privileged Scaffolds for Library Design and Drug Discovery. *Curr. Opin. Chem. Biol.* **2010,** *14*, 347-361.

2. Löber, S.; Hübner, H.; Tschammer, N.; Gmeiner, P. Recent Advances in the Search for D3- and D4-Selective Drugs: Probes, Models and Candidates. *Trends Pharmacol. Sci.* **2011,** *32*, 148-157.

3. Szabo, M.; Klein Herenbrink, C.; Christopoulos, A.; Lane, J. R.; Capuano, B. Structure–Activity Relationships of Privileged Structures Lead to the Discovery of Novel Biased Ligands at the Dopamine D2 Receptor. *J. Med. Chem.* **2014,** *57*, 4924-4939.

4. Newman, A. H.; Beuming, T.; Banala, A. K.; Donthamsetti, P.; Pongetti, K.; LaBounty, A.; Levy, B.; Cao, J.; Michino, M.; Luedtke, R. R.; Javitch, J. A.; Shi, L. Molecular Determinants of Selectivity and Efficacy at the Dopamine D3 Receptor. *J. Med. Chem.* **2012,** *55*, 6689-6699.

5. Ehrlich, K.; Götz, A.; Bollinger, S.; Tschammer, N.; Bettinetti, L.; Härterich, S.; Hübner, H.; Lanig, H.; Gmeiner, P. Dopamine D2, D3, and D4 Selective Phenylpiperazines as Molecular Probes to Explore the Origins of Subtype Specific Receptor Binding. *J. Med. Chem.* **2009,** *52*, 4923-4935.

6. Burris, K. D.; Molski, T. F.; Xu, C.; Ryan, E.; Tottori, K.; Kikuchi, T.; Yocca, F. D.; Molinoff, P. B. Aripiprazole, a Novel Antipsychotic, Is a High-Affinity Partial Agonist at Human Dopamine D2 Receptors. *J. Pharmacol. Exp. Ther.* **2002,** *302*, 381-389.

7. Kiss, B.; Horvath, A.; Nemethy, Z.; Schmidt, E.; Laszlovszky, I.; Bugovics, G.; Fazekas, K.; Hornok, K.; Orosz, S.; Gyertyan, I.; Agai-Csongor, E.; Domany, G.; Tihanyi, K.; Adham, N.; Szombathelyi, Z. Cariprazine (RGH-188), a Dopamine D3 Receptor-Preferring, D3/D2 Dopamine Receptor Antagonist-Partial Agonist Antipsychotic Candidate: In Vitro and Neurochemical Profile. *J. Pharmacol. Exp. Ther.* **2010,** *333*, 328-340.

8. Maeda, K.; Sugino, H.; Akazawa, H.; Amada, N.; Shimada, J.; Futamura, T.; Yamashita, H.; Ito, N.; McQuade, R. D.; Mørk, A.; Pehrson, A. L.; Hentzer, M.; Nielsen, V.; Bundgaard, C.; Arnt, J.; Stensbøl, T. B.; Kikuchi, T. Brexpiprazole I: In Vitro and in Vivo Characterization of a Novel Serotonin-Dopamine Activity Modulator. *J. Pharmacol. Exp. Ther.* **2014,** *350*, 589.

9. Citrome, L. The ABC's of Dopamine Receptor Partial Agonists – Aripiprazole, Brexpiprazole and Cariprazine: The 15-Min Challenge to Sort These Agents Out. *Int. J. Clin. Pract.* **2015,** *69*, 1211-1220.

10. Möller, D.; Kling, R. C.; Skultety, M.; Leuner, K.; Hübner, H.; Gmeiner, P. Functionally Selective Dopamine D2, D3 Receptor Partial Agonists. *J. Med. Chem.* **2014,** *57*, 4861-4875.

11. Allen, J. A.; Yost, J. M.; Setola, V.; Chen, X.; Sassano, M. F.; Chen, M.; Peterson, S.; Yadav, P. N.; Huang, X. P.; Feng, B.; Jensen, N. H.; Che, X.; Bai, X.; Frye, S. V.; Wetsel, W. C.; Caron, M. G.; Javitch, J. A.; Roth, B. L.; Jin, J. Discovery of Beta-Arrestin-Biased Dopamine D2 Ligands for Probing Signal Transduction Pathways Essential for Antipsychotic Efficacy. *Proc. Natl. Acad. Sci. U. S. A.* **2011,** *108*, 18488-18493.

12. Chen, X.; McCorvy, J. D.; Fischer, M. G.; Butler, K. V.; Shen, Y.; Roth, B. L.; Jin, J. Discovery of G Protein-Biased D2 Dopamine Receptor Partial Agonists. *J. Med. Chem.* **2016,** *59*, 10601-10618.

13. Chen, X.; Sassano, M. F.; Zheng, L.; Setola, V.; Chen, M.; Bai, X.; Frye, S. V.; Wetsel, W. C.; Roth, B. L.; Jin, J. Structure-Functional Selectivity Relationship Studies of Beta-Arrestin-Biased Dopamine D2 Receptor Agonists. *J. Med. Chem.* **2012,** *55*, 7141-7153.

14. Shonberg, J.; Herenbrink, C. K.; Lopez, L.; Christopoulos, A.; Scammells, P. J.; Capuano, B.; Lane, J. R. A Structure-Activity Analysis of Biased Agonism at the Dopamine D2 Receptor. *J. Med. Chem.* **2013,** *56*, 9199-9221.

15. Costa-Neto, C. M.; Parreiras-e-Silva, L. T.; Bouvier, M. A Pluridimensional View of Biased Agonism. *Mol. Pharmacol.* **2016,** *90*, 587-595.

16. Galandrin, S.; Oligny-Longpré, G.; Bouvier, M. The Evasive Nature of Drug Efficacy: Implications for Drug Discovery. *Trends Pharmacol. Sci.* **2007,** *28*, 423-430.

17. Bock, A.; Kostenis, E.; Tränkle, C.; Lohse, M. J.; Mohr, K. Pilot the Pulse: Controlling the Multiplicity of Receptor Dynamics. *Trends Pharmacol. Sci.* **2014,** *35*, 630-638.

18. Lane, J. R.; Donthamsetti, P.; Shonberg, J.; Draper-Joyce, C. J.; Dentry, S.; Michino, M.; Shi, L.; López, L.; Scammells, P. J.; Capuano, B.; Sexton, P. M.; Javitch, J. A.; Christopoulos, A. A New Mechanism of Allostery in a G Protein–Coupled Receptor Dimer. *Nat. Chem. Biol.* **2014,** *10*, 745-752.

19. Weichert, D.; Banerjee, A.; Hiller, C.; Kling, R. C.; Hübner, H.; Gmeiner, P. Molecular Determinants of Biased Agonism at the Dopamine D2 Receptor. *J. Med. Chem.* **2015,** *58*, 2703-2717.

20. Cannon, J. G. Structure-Activity Relationships of Dopamine Agonists. *Annu. Rev. Pharmacol. Toxicol.* **1983,** *23*, 103-129.

21. Masri, B.; Salahpour, A.; Didriksen, M.; Ghisi, V.; Beaulieu, J. M.; Gainetdinov, R. R.; Caron, M. G. Antagonism of Dopamine D2 Receptor/Beta-Arrestin 2 Interaction Is a Common Property of Clinically Effective Antipsychotics. *Proc. Natl. Acad. Sci. U. S. A.* **2008,** *105*, 13656-13661.

22. Sandanayaka, V., Singh, J., Zhou, L.-M., Gurney, M.E. Biaryl Nitrogen-Heterocycle Inhibitors of LTA4H for Treating Inflammation. US2007/0149544 A1, 2007.

23. Möller, D.; Salama, I.; Kling, R. C.; Hübner, H.; Gmeiner, P. 1,4-Disubstituted Aromatic Piperazines with High 5-HT2a/D2 Selectivity: Quantitative Structure-Selectivity Investigations, Docking, Synthesis and Biological Evaluation. *Biorg. Med. Chem.* **2015,** *23*, 6195-6209.

24. Kendall, J. D.; Marshall, A. J. Pyrazolo[1,5-a]Pyridine Derivatives as PI3 Kinase Inhibitors and Their Preparation, Pharmaceutical Compositions and Use in the Treatment of Cancers. WO2009008748A1, 2009.

25. Gmeiner, P.; Huebner, H.; Skultety, M. Preparation of Indolizines and Aza-Analog Derivatives Thereof as CNS Active Compounds. WO2008113559A2, 2008.

26. Boeckler, F.; Ohnmacht, U.; Lehmann, T.; Utz, W.; Hübner, H.; Gmeiner, P. COMFA and COMSIA Investigations Revealing Novel Insights into the Binding Modes of Dopamine D3 Receptor Agonists. *J. Med. Chem.* **2005,** *48*, 2493-2508.

27. Moffett, R. B.; Hanze, A. R.; Seay, P. H. Central Nervous System Depressants. V. Polyhydroxy and Methoxyphenyl Ketones, Carbinols, and Derivatives. *J. Med. Chem.* **1964,** *7*, 178-186.

28. De Luca, L.; Giacomelli, G.; Porcheddu, A. Beckmann Rearrangement of Oximes under Very Mild Conditions. *J. Org. Chem.* **2002,** *67*, 6272-6274.

29. Dulcere, J. P. Vilsmeier Reagent for a High-Yield Conversion of Aldoximes to Nitriles. *Tetrahedron Lett.* **1981,** *22*, 1599-1600.

30. Lane, J. R.; Powney, B.; Wise, A.; Rees, S.; Milligan, G. G Protein Coupling and Ligand Selectivity of the D2L and D3 Dopamine Receptors. *J. Pharmacol. Exp. Ther.* **2008,** *325*, 319-330.

31. Gazi, L. N., S.; Strange P.G. Functional Coupling of the Human Dopamine D2 Receptor with Galphai1, Galphai2, Galphai3, and Galphao G Proteins: Evidence for Agonist Regulation of G Protein Selectivity. *Br. J. Pharmacol.* **2003,** *138*, 775-786.

32. Ahlgren-Beckendorf, J. A.; Levant, B. Signaling Mechanisms of the D3 Dopamine Receptor. *J. Recept. Signal Transduction* **2004,** *24*, 117-130.

33. Jiang, M.; Spicher, K.; Boulay, G.; Wang, Y.; Birnbaumer, L. Most Central Nervous System D2 Dopamine Receptors Are Coupled to Their Effectors by Go. *Proc. Natl. Acad. Sci. U. S. A.* **2001,** *98*, 3577-3582.

34. Asano, T.; Morishita, R.; Semba, R.; Itoh, H.; Kaziro, Y.; Kato, K. Identification of Lung Major Gtp-Binding Protein as Gi2 and Its Distribution in Various Rat-Tissues Determined by Immunoassay. *Biochemistry* **1989,** *28*, 4749-4754.

35. Strange, P. G. Use of the Gtpgammas Binding Assay for Analysis of Ligand Potency and Efficacy at G Protein-Coupled Receptors. *Br. J. Pharmacol.* **2010,** *161*, 1238-1249.

36. Harrison, C.; Traynor, J. R. The [35s]Gtpγs Binding Assay: Approaches and Applications in Pharmacology. *Life Sci.* **2003,** *74*, 489-508.

37. In *Assay Guidance Manual*, Sittampalam, G. S.; Coussens, N. P.; Nelson, H.; Arkin, M.; Auld, D.; Austin, C.; Bejcek, B.; Glicksman, M.; Inglese, J.; Iversen, P. W.; Li, Z.; McGee, J.; McManus, O.; Minor, L.; Napper, A.; Peltier, J. M.; Riss, T.; Trask, O. J., Jr.; Weidner, J., Eds. Eli Lilly & Company and the National Center for Advancing Translational Sciences: Bethesda MD, 2004.

38. Klein Herenbrink, C.; Sykes, D. A.; Donthamsetti, P.; Canals, M.; Coudrat, T.; Shonberg, J.; Scammells, P. J.; Capuano, B.; Sexton, P. M.; Charlton, S. J.; Javitch, J. A.; Christopoulos, A.; Lane, J. R. The Role of Kinetic Context in Apparent Biased Agonism at GPCRs. *Nat. Commun.* **2016,** *7*, 10842.

39. Gales, C.; Rebois, R. V.; Hogue, M.; Trieu, P.; Breit, A.; Hebert, T. E.; Bouvier, M. Real-Time Monitoring of Receptor and G-Protein Interactions in Living Cells. *Nat. Methods* **2005,** *2*, 177-184.

40. Richard-Lalonde, M.; Nagi, K.; Audet, N.; Sleno, R.; Amraei, M.; Hogue, M.; Balboni, G.; Schiller, P. W.; Bouvier, M.; Hébert, T. E.; Pineyro, G. Conformational Dynamics of Kir3.1/Kir3.2 Channel Activation Via δ-Opioid Receptors. *Mol. Pharmacol.* **2013,** *83*, 416-428.

41. Quoyer, J.; Janz, J. M.; Luo, J.; Ren, Y.; Armando, S.; Lukashova, V.; Benovic, J. L.; Carlson, K. E.; Hunt, S. W.; Bouvier, M. Pepducin Targeting the C-X-C Chemokine Receptor Type 4 Acts as a Biased Agonist Favoring Activation of the Inhibitory G Protein. *Proc. Natl. Acad. Sci. U. S. A.* **2013,** *110*, E5088-E5097.

42. Gales, C.; Van Durm, J. J. J.; Schaak, S.; Pontier, S.; Percherancier, Y.; Audet, M.; Paris, H.; Bouvier, M. Probing the Activation-Promoted Structural Rearrangements in Preassembled Receptor-G Protein Complexes. *Nat. Struct. Mol. Biol.* **2006,** *13*, 778-786.

43. Black, J. W.; Leff, P. Operational Models of Pharmacological Agonism. *Proc. R. Soc. London, Ser. B* **1983,** *220*, 141-162.

44. Kenakin, T.; Watson, C.; Muniz-Medina, V.; Christopoulos, A.; Novick, S. A Simple Method for Quantifying Functional Selectivity and Agonist Bias. *ACS Chem. Neurosci.* **2012,** *3*, 193-203.

45. van der Westhuizen, E. T.; Breton, B.; Christopoulos, A.; Bouvier, M. Quantification of Ligand Bias for Clinically Relevant B2-Adrenergic Receptor Ligands: Implications for Drug Taxonomy. *Mol. Pharmacol.* **2014,** *85*, 492-509.

46. Shonberg, J.; Lopez, L.; Scammells, P. J.; Christopoulos, A.; Capuano, B.; Lane, J. R. Biased Agonism at G Protein-Coupled Receptors: The Promise and the Challenges - a Medicinal Chemistry Perspective. *Med. Res. Rev.* **2014,** *34*, 1286-330.

47. Kenakin, T.; Christopoulos, A. Signalling Bias in New Drug Discovery: Detection, Quantification and Therapeutic Impact. *Nat. Rev. Drug Discovery* **2013,** *12*, 205-216.

48. Namkung, Y.; Le Gouill, C.; Lukashova, V.; Kobayashi, H.; Hogue, M.; Khoury, E.; Song, M.; Bouvier, M.; Laporte, S. A. Monitoring G Protein-Coupled Receptor and Beta-Arrestin Trafficking in Live Cells Using Enhanced Bystander Bret. *Nat. Commun.* **2016,** *7*, 12178.

49. Luján, R.; Marron Fernandez de Velasco, E.; Aguado, C.; Wickman, K. New Insights into the Therapeutic Potential of Girk Channels. *Trends Neurosci.* **2014,** *37*, 20-29.

50. Lüscher, C.; Slesinger, P. A. Emerging Concepts for G Protein-Gated Inwardly Rectifying Potassium (GIRK) Channels in Health and Disease. *Nat. Rev. Neurosci.* **2010,** *11*, 301-315.

51. Whorton, M. R.; MacKinnon, R. X-Ray Structure of the Mammalian GIRK2-Beta Gamma G-Protein Complex. *Nature* **2013,** *498*, 190-197.

52. Yamada, K.; Iwayama, Y.; Toyota, T.; Ohnishi, T.; Ohba, H.; Maekawa, M.; Yoshikawa, T. Association Study of the Kcnj3 Gene as a Susceptibility Candidate for Schizophrenia in the Chinese Population. *Hum. Genet.* **2012,** *131*, 443-451.

53. Yamada, K.; Iwayama, Y.; Hattori, E.; Iwamoto, K.; Toyota, T.; Ohnishi, T.; Ohba, H.; Maekawa, M.; Kato, T.; Yoshikawa, T. Genome-Wide Association Study of Schizophrenia in Japanese Population. *PLoS ONE* **2011,** *6*, e20468.

54. Farhy Tselnicker, I.; Tsemakhovich, V.; Rishal, I.; Kahanovitch, U.; Dessauer, C. W.; Dascal, N. Dual Regulation of G Proteins and the G-Protein–Activated K+ Channels by Lithium. *Proc. Natl. Acad. Sci. U. S. A.* **2014,** *111*, 5018-5023.

55. Kuzhikandathil, E. V.; Yu, W.; Oxford, G. S. Human Dopamine D3 and D2L Receptors Couple to Inward Rectifier Potassium Channels in Mammalian Cell Lines. *Mol. Cell. Neurosci.* **1998,** *12*, 390-402.

56. Lavine, N.; Ethier, N.; Oak, J. N.; Pei, L.; Liu, F.; Trieu, P.; Rebois, R. V.; Bouvier, M.; Hébert, T. E.; Van Tol, H. H. M. G Protein-Coupled Receptors Form Stable Complexes with Inwardly Rectifying Potassium Channels and Adenylyl Cyclase. *J. Biol. Chem.* **2002,** *277*, 46010-46019.

57. Heusler, P.; Newman-Tancredi, A.; Castro-Fernandez, A.; Cussac, D. Differential Agonist and Inverse Agonist Profile of Antipsychotics at D2L Receptors Coupled to GIRK Potassium Channels. *Neuropharmacology* **2007,** *52*, 1106-1113.

58. Shapiro, D. A.; Renock, S.; Arrington, E.; Chiodo, L. A.; Liu, L.-X.; Sibley, D. R.; Roth, B. L.; Mailman, R. Aripiprazole, a Novel Atypical Antipsychotic Drug with a Unique and Robust Pharmacology. *Neuropsychopharmacology* **2003,** *28*, 1400-1411.

59. Klose, A.; Huth, T.; Alzheimer, C. 1-[6-[[(17β)-3-Methoxyestra-1,3,5(10)-Trien-17-Yl]Amino]Hexyl]-1h-Pyrrole-2,5-Dione (U73122) Selectively Inhibits Kir3 and Bk Channels in a Phospholipase C-Independent Fashion. *Mol. Pharmacol.* **2008,** *74*, 1203-1214.

60. Liao, Y. J.; Jan, Y. N.; Jan, L. Y. Heteromultimerization of G-Protein-Gated Inwardly Rectifying K+ Channel Proteins GIRK1 and GIRK2 and Their Altered Expression in Weaver Brain. *J. Neurosci.* **1996,** *16*, 7137-7150.

61. Tenn, C. C.; Fletcher, P. J.; Kapur, S. A Putative Animal Model of the "Prodromal" State of Schizophrenia. *Biol. Psychiatry* **2005,** *57*, 586-593.

62. Peleg-Raibstein, D.; Sydekum, E.; Feldon, J. Differential Effects on Prepulse Inhibition of Withdrawal from Two Different Repeated Administration Schedules of Amphetamine. *Int. J. Neuropsychopharmacol.* **2006,** *9*, 737-749.

63. Cancela, L. M.; Basso, A. M.; Martijena, I. D.; Capriles, N. R.; Molina, V. A. A Dopaminergic Mechanism Is Involved in the 'Anxiogenic-Like' Response Induced by Chronic Amphetamine Treatment: A Behavioral and Neurochemical Study. *Brain Res.* **2001,** *909*, 179-186.

64. Amato, D.; Pum, M. E.; Groos, D.; Lauber, A. C.; Huston, J. P.; Carey, R. J.; de Souza Silva, M. A.; Müller, C. P. Neuropharmacology of Light-Induced Locomotor Activation. *Neuropharmacology* **2015,** *95*, 243-251.

65. Pum, M. E.; Huston, J. P.; Müller, C. P.; De Souza Silva, M. A. Light-Induced Activity in the Activity Box Is Not Aversively Motivated and Does Not Show between-Trial Habituation. *Physiol. Behav.* **2009,** *96*, 434-439.

66. Pum, M. E.; Huston, J. P.; De Souza Silva, M. A.; Müller, C. P. Visual Sensory-Motor Gating by Serotonin Activation in the Medial Prefrontal and Occipital, but not in the Rhinal, Cortices in Rats. *Neuroscience* **2008,** *153*, 361-372.

67. Featherstone, R. E.; Kapur, S.; Fletcher, P. J. The Amphetamine-Induced Sensitized State as a Model of Schizophrenia. *Prog. Neuro-Psychopharmacol. Biol. Psychiatry* **2007,** *31*, 1556-1571.

68. Prut, L.; Belzung, C. The Open Field as a Paradigm to Measure the Effects of Drugs on Anxiety-Like Behaviors: A Review. *Eur. J. Pharmacol.* **2003,** *463*, 3-33.

69. Antelman, S. M.; Chiodo, L. A. Amphetamine as a Stressor. In *Stimulants: Neurochemical, Behavioral and Clinical Perspectives*, Cresse, I., Ed. Raven Press: New York, 1983; pp 269-299.

70. Braga, R. J.; Petrides, G.; Figueira, I. Anxiety Disorders in Schizophrenia. *Compr. Psychiatry* **2004,** *45*, 460-468.

71. Buckley, P. F.; Miller, B. J.; Lehrer, D. S.; Castle, D. J. Psychiatric Comorbidities and Schizophrenia. *Schizophr. Bull.* **2009,** *35*, 383-402.

72. Shin, H.-W.; Chung, S. J. Drug-Induced Parkinsonism. *J. Clin. Neurol.* **2012,** *8*, 15-21.

73. Leucht, S.; Wahlbeck, K.; Hamann, J.; Kissling, W. New Generation Antipsychotics Versus Low-Potency Conventional Antipsychotics: A Systematic Review and Meta-Analysis. *Lancet* **2003,** *361*, 1581-1589.

74. Robinson, T. E.; Becker, J. B. Enduring Changes in Brain and Behavior Produced by Chronic Amphetamine Administration: A Review and Evaluation of Animal Models of Amphetamine Psychosis. *Brain Res. Rev.* **1986,** *11*, 157-198.

75. Tschammer, N.; Elsner, J.; Goetz, A.; Ehrlich, K.; Schuster, S.; Ruberg, M.; Kuhhorn, J.; Thompson, D.; Whistler, J.; Hubner, H.; Gmeiner, P. Highly Potent 5-Aminotetrahydropyrazolopyridines: Enantioselective Dopamine D3 Receptor Binding, Functional Selectivity, and Analysis of Receptor-Ligand Interactions. *J. Med. Chem.* **2011,** *54*, 2477-2491.

76. Lowry, O. H.; Rosebrough, N. J.; Farr, A. L.; Randall, R. J. Protein Measurement with the Folin Phenol Reagent. *J. Biol. Chem.* **1951,** *193*, 265-275.

77. Hübner, H.; Haubmann, C.; Utz, W.; Gmeiner, P. Conjugated Enynes as Nonaromatic Catechol Bioisosteres: Synthesis, Binding Experiments, and Computational Studies of Novel Dopamine Receptor Agonists Recognizing Preferentially the D3 Subtype. *J. Med. Chem.* **2000,** *43*, 756-762.

78. Cheng, Y.-C.; Prusoff, W. H. Relationship between the Inhibition Constant (Ki) and the Concentration of Inhibitor Which Causes 50 Per Cent Inhibition (I50) of an Enzymatic Reaction. *Biochem. Pharmacol.* **1973,** *22*, 3099-3108.

79. Namkung, Y.; Radresa, O.; Armando, S.; Devost, D.; Beautrait, A.; Le Gouill, C.; Laporte, S. A. Quantifying Biased Signaling in Gpcrs Using Bret-Based Biosensors. *Methods* **2016,** *92*, 5-10.

80. Amato, D.; Natesan, S.; Yavich, L.; Kapur, S.; Müller, C. P. Dynamic Regulation of Dopamine and Serotonin Responses to Salient Stimuli During Chronic Haloperidol Treatment. *Int. J. Neuropsychopharmacol.* **2011,** *14*, 1327-1339.

TABLE OF CONTENTS GRAPHIC